

# **Droplet Shapes for a Class of Models in $\mathbb{Z}^2$ at Zero Temperature**

**Xavier Descombes<sup>1</sup> and Eugène Pechersky<sup>2</sup>**

*Received February 12, 2002; accepted June 28, 2002*

---

In this work we consider the Wulff construction at zero temperature for a class of Gibbs models and study the shape of the obtained droplets. Considering zero temperature we avoid all difficulties connected with the competition between energy and entropy. It allows us to study a quite wide class of models which provides a variety of shapes. The motivations of the study come from attempts to describe isotropic properties of some models on 2D lattice at zero temperature. The studied models are binary (the spin space is 0, 1) with a ferromagnetic behavior such that the potential functions are not equal to zero only for some tiles with size  $3 \times 3$ . In fact, we study herein droplet shapes of a subclass of the ferromagnetic models with potential functions as mentioned above. This subclass of models is defined by a condition called regularity. We call the model classified here as having regular micro-boundaries. Several examples of non-regular models are also presented.

---

**KEY WORDS:** Canonical ensemble; droplet shape; Wulff construction.

## **1. INTRODUCTION**

There exists a quite large scope of texts dealing with droplets of one phase inside another one (see for example refs. 2–5). The main goal of the mentioned works is to prove the existence of a unique big contour separating

---

<sup>1</sup> Ariana, common project CNRS/INRIA/UNSA, 2004 route des Lucioles, BP 9306902, Sophia Antipolis Cedex, France; e-mail: Xavier.Descombes@sophia.inria.fr

<sup>2</sup> Institute of Information Transmission Problems, Russian AS, 19, Bolshoi Karetnyi, GSP-4, Moscow 101447, Russia; e-mail: pech@iitp.ru

the phases at a low positive temperature at the thermodynamical limit. All these studies concern a small set of models. In the first works<sup>(2, 3)</sup> and in the fundamental work<sup>(4)</sup> the Ising model was studied with this respect. These results have been extended in further works to the Potts model, the lattice gas models and several others.<sup>(5)</sup>

In the present work, we study the shape of the droplets at zero temperature. It permits to avoid all difficulties connected with the competition between energy and entropy. Therefore, it allows us to consider a wide class of models that leads to a diversity of droplet shapes.

The original motivation for this study comes from image processing. In the Gibbs field approach to image processing, the Gibbs field plays the role of a smoothing tool which is expected to decrease noise in the resulting image. For example, in the segmentation problem, where the resulting image is a partition of an original image into regions of different textures, a model defined by a Gibbs field with ferromagnetic interaction smoothes the region boundaries. Obviously, this smoothing property must not depend on the angle of boundary slopes to the co-ordinate systems. That is, the energy of interaction over boundaries should be isotropic. However it is improbable to have such an isotropy property on the two dimension lattice where digitized images are usually presented. On the other hand, it is reasonable, considering the computation point of view, to use finite range models, which are surely not isotropic. It is clear that different models can have different "degree" of isotropy. One of our goals is to describe the isotropy degree of binary models. In order to describe the isotropy we propose the droplet shape as a measure of the model isotropy. Deviations of the droplet shapes from the circle measured in one or another way may serve as an isotropy degree.

In this work we study the droplet shapes for a subclass of binary ferromagnetic models on  $\mathbb{Z}^2$  with potential functions of range less than or equal to  $2\sqrt{2}$ . We give a classification of the mentioned models with respect to their droplet shapes. The subclass of ferromagnetic models is determined by a condition referred to as regularity. The main result describes a set of polygons representing the droplet shapes in the thermodynamical limit at zero temperature. In particular, the set includes the square which is well known for the Ising model, and a sixteen-edges polygon (non-regular) obtained for the model described in ref. 10. For the regular models, only two parameters, depending on the model potential, completely determine the corresponding polygon.

We conjecture that the same zoo of polygons gives the droplet shapes for all ferromagnetic models with range  $2\sqrt{2}$ . However, we do not study in this work the total set of these models. It seems that such an investigation requires a lot of combinatorics.

The polygons discussed here are the droplet shapes at the thermodynamical limit. We call these shapes the droplet shapes on macro-level or macro-level shapes. There is a great multiplicity of boundary structures of prelimiting droplets even at zero temperature. Prelimiting droplet shapes may not be convex. Moreover, in one of examples (see Example 3 in Section 4.1) of a non-regular model the droplet boundary is not connected. The regularity condition allows us to avoid such exotic cases.

In Sections 2 and 3 we formulate and prove our main result concerning the classification of regular models. Section 4 contains several examples of non-regular models and a discussion about conditions of the regularity. Parts of the main theorem proof are very technical and postponed to the Appendix.

## 2. MODEL DESCRIPTION AND MAIN RESULTS

### 2.1. $3 \times 3$ Models

We study models on  $\mathbb{Z}^2$  with the spin space  $X = \{0, 1\}$ . The only potential functions which can take non-zero values are

$$\Phi_{W_i}: X^{W_i} \rightarrow \mathbb{R}, \quad (1)$$

where

$$W_0 = \{t = (t_1, t_2) \in \mathbb{Z}^2 : |t_i| \leq 1, i = 1, 2\}, \quad (2)$$

and  $W_t = W_0 + t$ . A subset  $W_t$  is called a *plaquette*. We consider translation invariant models. Hence  $\Phi_{W_0}(\mathbf{x}) = \Phi_{W_t}(T_t \mathbf{x})$ , where  $T_t \mathbf{x}(u) = \mathbf{x}(t - u)$ , for any configuration  $\mathbf{x}: \mathbb{Z}^2 \rightarrow X$ , and any  $t \in \mathbb{Z}^2$ .

We consider the Gibbs distribution defined by  $\Phi$  in a standard way. Let  $\Theta \subset \mathbb{Z}^2$  be a finite volume and  $\mathcal{P}_\Theta$  be the set of all plaquettes in  $\Theta$ . Then the energy of any configuration  $\mathbf{x}: \Theta \rightarrow X$  is

$$H(\mathbf{x}) = \sum_{W \in \mathcal{P}_\Theta} \Phi(\mathbf{x}_W). \quad (3)$$

The Gibbs probability of  $\mathbf{x}$  in the volume  $\Theta$  is

$$P_{\Theta, \beta}(\mathbf{x}) = \frac{\exp\{-\beta H(\mathbf{x})\}}{Z_{\Theta, \beta}}, \quad (4)$$

where  $Z_{\theta, \beta} = \sum_{\mathbf{y} \in X^\theta} \exp\{-\beta H(\mathbf{y})\}$ . The Gibbs distribution in  $\mathbb{Z}^2$  is defined by the thermodynamical limit of the specification (4). Further we use a different form of the thermodynamical limit for a specification with boundary conditions. The definition will be given later.

Next we give the main assumptions on  $\Phi$ . A *tile* is a table of nine numbers:

$$\bar{r} = \begin{pmatrix} r_{11} & r_{12} & r_{13} \\ r_{21} & r_{22} & r_{23} \\ r_{31} & r_{32} & r_{33} \end{pmatrix}, \quad (5)$$

where  $r_{ij} \in \{0, 1\}$ . Let  $\bar{v}_0 = \begin{pmatrix} 0 & 0 & 0 \\ 0 & 0 & 0 \\ 0 & 0 & 0 \end{pmatrix}$  and  $\bar{v}_1 = \begin{pmatrix} 1 & 1 & 1 \\ 1 & 1 & 1 \\ 1 & 1 & 1 \end{pmatrix}$ . We center the values of  $\Phi$  by assuming that:

$$\Phi(\bar{v}_0) = \Phi(\bar{v}_1) = 0. \quad (6)$$

Generally there are  $2^9$  different tiles and the same number of different values of  $\Phi$ . However, we require  $\Phi$  to be invariant with respect to the natural tile symmetries. Namely, all rotations of  $\bar{r}$  by  $\frac{\pi}{2}$  and reflections with respect to horizontal and vertical axes generate a group  $\hat{G}$  of tile transformations. Besides we add to  $\hat{G}$  flips of  $\bar{r}$  taking every  $r_{ij}$  to  $1 + r_{ij} \pmod{2}$ . Let  $G$  be the complete group of the described transformations of  $\bar{r}$ .

We assume that the following conditions on the function  $\Phi$  are satisfied:

**\Phi1.** For any  $g \in G$  and any  $\bar{r}$

$$\Phi(\bar{r}) = \Phi(g(\bar{r})).$$

This condition reduces the  $2^9$  possible different values of  $\Phi$  to 51.

The next condition ensures that the models are of ferromagnetic type.

Let  $k_1, k_2 \in \mathbb{Z}_+$  be such that  $k_i \geq 3$ ,  $i = 1, 2$ . Consider a table  $\hat{s} = (s_{ij})_{\substack{1 \leq i \leq k_1, \\ 1 \leq j \leq k_2}}$ , where  $s_{ij} \in \{0, 1\}$ . Let  $\mathcal{T}_{\hat{s}} = \{\bar{r}\}$  be the set of all tiles  $\bar{r}$  which can be extracted from  $\hat{s}$ . We assume that:

**\Phi2.** If  $\hat{s}$  is not constant (0 or 1) then:

$$\sum_{\bar{r} \in \mathcal{T}_{\hat{s}}} \Phi(\bar{r}) > 0.$$

It follows from (6) and **\Phi2** that every local perturbation of the configuration  $\mathbf{x}_0(t) \equiv 0$  (or  $\mathbf{x}_0(t) \equiv 1$ ),  $t \in \mathbb{Z}^2$ , has a finite positive energy.

Therefore the configurations  $\mathbf{x}_0(t) \equiv 0$  and  $\mathbf{x}_1(t) \equiv 1$  are the only periodical ground states. Of course, there are infinite many nonperiodical ground states. It is also easy to see that the Peierls conditions are satisfied.<sup>(9, 8)</sup> Therefore, there exists a critical temperature separating the case of a unique Gibbs state and the case of two (at least) Gibbs states.

We use the thermodynamical limit in the following form. Let  $A = \{\lambda = (\lambda_1, \lambda_2) \in \mathbb{R}^2 : |\lambda_i| \leq 1, i = 1, 2\}$  be the square in  $\mathbb{R}^2$  and let  $\frac{1}{n}\mathbb{Z}^2 \subset \mathbb{R}^2$  be the natural embedding of the lattice  $\mathbb{Z}^2$ , scaled by  $\frac{1}{n}$ , into  $\mathbb{R}^2$ . Let  $A_n = A \cap \frac{1}{n}\mathbb{Z}^2$ . The  $p$ -boundary of  $A_n$  is  $\partial A_n = \{t \in A_n^c : \text{dist}(t, A_n) \leq \frac{2\sqrt{2}}{n}\}$  and  $\hat{A}_n = A_n \cup \partial A_n$ . We use the term  $p$ -boundary to outline the difference with the usual definition of boundary. Denote by  $\mathbf{X}_n = X^{A_n}$  the set of all configurations on  $A_n$ . We use the notation  $P_n(\mathbf{x})$  for the Gibbs distribution on  $\mathbf{X}_n$  generated by  $P_{\theta, \beta}$  (see Eq. (4)).

Further we study the canonical ensemble with boundary conditions. Therefore all configurations are extended out of  $A_n$ . We consider the only boundary condition such that  $\mathbf{x}(t) = 1$  for  $t \notin A_n$ . The canonical ensemble is a Gibbs distribution defined on  $\frac{1}{n}\mathbb{Z}^2$  as follows. Let  $D_1, D_2$  be positive constants,  $\gamma \in (0, 1)$ . Consider the set:

$$\hat{\mathbf{X}}_n^\gamma = \left\{ \mathbf{x} \in \mathbf{X}_n : \gamma - \frac{D_1}{n} \leq \frac{|\mathbf{x}|}{(2n+1)^2} \leq \gamma + \frac{D_2}{n} \right\},$$

where  $|\mathbf{x}|$  is the number of sites in  $A_n$  equal to 0, and  $\mathbf{X}_n^\gamma$  is the subset of  $X_n^{\frac{1}{n}\mathbb{Z}^2}$  such that every configuration of  $\mathbf{X}_n^\gamma$  is a configuration of  $\hat{\mathbf{X}}_n^\gamma$  extended by 1's out of  $A_n$ . Then the Gibbs distribution  $P_n^\gamma(\cdot)$  of the canonical ensemble on  $\mathbf{X}_n^\gamma$  with the introduced boundary condition is

$$P_n^\gamma(A) = \frac{\sum_{\mathbf{x} \in A} \exp\{-\beta H(\mathbf{x})\}}{Z_n^\gamma}, \tag{7}$$

where  $A \subseteq \mathbf{X}_n^\gamma$ ,  $Z_n^\gamma = \sum_{\mathbf{x} \in \mathbf{X}_n^\gamma} \exp\{-\beta H(\mathbf{x})\}$  and  $H$  is the Hamiltonian of the model corresponding to  $\Phi$ .

For any model of the considered class and every  $n$ , let  $\mathbf{Y}_n^\gamma \subseteq \mathbf{X}_n^\gamma$  be the set of all configurations having minimal energy. We call every configuration of  $\mathbf{Y}_n^\gamma$  a *ground state* of the canonical ensemble or simply a ground state. We use the same term *ground state* for both the canonical ensemble and the grand ensemble, however it will not cause confusion. The simple lemma below shows that any configuration of  $\mathbf{Y}_n^\gamma$  has a droplet composed of 0's. In order to avoid problems arising because of boundary effects we consider the case where  $\gamma$  is small enough.

Next, we introduce several notions. If  $\mathbf{x} \in \mathbf{X}_n$  then the set  $\Omega_{\mathbf{x}}(0) = \{t \in \bar{A}_n : \mathbf{x}_{W_t} \equiv 0\}$  is called the *0-phase* of  $\mathbf{x}$  and the set  $\Omega_{\mathbf{x}}(1) = \{t \in \bar{A}_n : \mathbf{x}_{W_t} \equiv 1\}$  is called the *1-phase* of  $\mathbf{x}$ . The *p-contour*  $\Omega_{\mathbf{x}} = \bar{A}_n \setminus (\Omega_{\mathbf{x}}(0) \cup \Omega_{\mathbf{x}}(1))$  of  $\mathbf{x}$  is the subset of sites in  $\bar{A}_n$  such that  $\mathbf{x}_{W_t}$  is not constant. We use the term *p-contour* because later we shall use the term *contour* in the usual sense of bonds with different configuration values on its ends.

**Lemma 1.** There exists positive constants  $C_1$  and  $C_2$  such that for large  $n$  and for any  $\mathbf{x} \in \mathbf{Y}_n^\gamma$  we have:

$$C_1 n \leq |\Omega_{\mathbf{x}}| \leq C_2 n.$$

Therefore there exists a constant  $C_0 > 0$  such that:  $|\Omega_{\mathbf{x}}(0)| > C_0 n^2$  for any  $\mathbf{x} \in \mathbf{Y}_n^\gamma$ .

*Proof.* It is easy to understand that

$$\liminf_{n \rightarrow \infty} \frac{|\Omega_{\mathbf{x}}|}{n} > 0.$$

This gives the left inequality. The upper bound can be proved by considering the following configuration:

$$\mathbf{y}(t) = \begin{cases} 0, & \text{if } \max\{|t_1|, |t_2|\} \leq \frac{m}{n}, \\ 1, & \text{otherwise,} \end{cases}$$

where  $\gamma - \frac{D_1}{n} \leq \frac{(2m+1)^2}{(2n+1)^2} \leq \gamma + \frac{D_2}{n}$ . Let  $\Gamma_0 = \{(t_1, t_2); 0 \leq t_1 \leq k_1, 0 \leq t_2 \leq k_2\}$  and  $\Gamma_t = \Gamma_0 + t$ . Let also  $k = |\{t: \Gamma_0 + t \supseteq W_0\}|$ . It follows from **\Phi 2** that:

$$\alpha_* = \frac{1}{k} \min\{H(\mathbf{x}_{\Gamma_0}) : \mathbf{x}_{\Gamma_0} \text{ is not a constant}\} > 0.$$

Let  $\alpha^* = \max_{\bar{r}}\{\Phi(\bar{r})\}$ . There exists  $\tilde{C}_2 > 0$  such that  $|\Omega_{\mathbf{y}}| \alpha^* \leq \tilde{C}_2 n$ . Since  $\mathbf{x} \in \mathbf{Y}_n^\gamma$  we have:

$$|\Omega_{\mathbf{x}}| \alpha_* \leq H(\mathbf{x}) \leq H(\mathbf{y}) \leq |\Omega_{\mathbf{y}}| \alpha^* \leq \tilde{C}_2 n.$$

Hence  $|\Omega_{\mathbf{x}}| \leq C_2 n$ , with  $C_2 = \frac{\tilde{C}_2}{\alpha_*}$ . ■

Two sites  $t_1, t_2 \in \frac{1}{n}\mathbb{Z}^2$  are *p-neighbors* if  $t_2 \in W_{t_1}$  or equivalently if  $t_1 \in W_{t_2}$ . A set  $\Delta \subseteq \frac{1}{n}\mathbb{Z}^2$  is *p-connected* if for any pair  $t_1, t_2 \in \Delta$  there exists a way of sites in  $\Delta$  being a sequence of *p-neighbors* linking  $t_1$  and  $t_2$ . The

0-phase  $\Omega_x(0)$  of  $\mathbf{x}$  is divided into  $p$ -connected components. Observe that the partition  $\Omega_x(0)$  into connected components, in conventional geometrical sense, gives the same set of components.

Any  $p$ -connected components of  $\Omega_x(0)$  is called a *micro-droplet*.

Let  $\mathbf{x} \in \mathbf{Y}_n^\gamma$ . It follows from Lemma 1 that  $\mathbf{x}$  has a micro-droplet with boundary length of order  $n$ . Since  $\mathbf{x}$  is a ground state of the canonical ensemble it is the only micro-droplet. This micro-droplet and the potential function  $\Phi$  have the same properties of invariance (see  $\Phi 1$ ).

Next we introduce the notion of *macro-droplet* following ref. 4. We map any configuration  $\mathbf{x} \in \mathbf{X}_n$ , to a measure  $\mu_x$  defined on  $\mathcal{A}$  in the following way:

$$\mu_x = \frac{1}{(2n+1)^2} \sum_{t \in \mathcal{A}_n} \mathbf{x}(t) \delta_t, \tag{8}$$

where  $\delta_t$  is the unique atom at  $t$ . This map generates distributions on the set of all measures  $\mu_x$  by the Gibbs distribution (4). We use the same symbol  $P_n$  for the generated distribution on the set  $M_n = \{\mu_x : \mathbf{x} \in X^{\mathcal{A}_n}\}$ . The map (8) generates also a distribution  $P_n^\gamma$  on  $M_n = \{\mu_x : \mathbf{x} \in \mathbf{X}_n^\gamma\}$  (see (7)). Recall that for  $\mathbf{x} \in \mathbf{X}_n^\gamma$  the measure  $\mu_x$  is formally defined on  $\mathbb{R}^2$  but its support is in  $\mathcal{A}$ .

Let  $(\mathbf{x}_n)$  be a sequence of configurations of  $\mathbf{X}_n^\gamma$ . The corresponding sequence of measures  $(\mu_{\mathbf{x}_n})$  is compact in  $M_n$  since their support is the compact set  $\mathcal{A}$ . Let  $\mu$  be a limiting measure of  $(\mu_{\mathbf{x}_n})$ . We say that  $\Delta \subseteq \mathcal{A}$  is a *macro-droplet* for  $\mu$  if

1.  $\mu(\Delta) = 0$ ,
2.  $|\Delta| > 0$ ,
3.  $\overset{\circ}{\Delta} = \Delta$ , where  $\bar{\Delta}$  is closure of  $\Delta$  and  $\overset{\circ}{\Delta}$  is interior of  $\bar{\Delta}$ .
4.  $|\Delta'| = |\Delta|$  for any  $\Delta' \supseteq \Delta$  satisfying 1.

If  $\mathbf{x}_n \in \mathbf{Y}_n^\gamma$  then any limiting measure  $\mu$  has an unique macro-droplet.

Our goal is to find the ground state of the models satisfying the conditions  $\Phi 1$  and  $\Phi 2$  for the canonical ensemble. We study the shape of the droplets and give a classification of the models with respect to the macro-droplet shape. Our proof is not extended to the whole class of models with  $\Phi 1$  and  $\Phi 2$ . We consider a subset of the whole class of models defined above referred as *regular* models. Nevertheless we think that a similar classification can be given for all models satisfying  $\Phi 1$  and  $\Phi 2$ .

## 2.2. Main Result

Consider the following tiles:

$$\begin{aligned} \bar{u}_0 &= \begin{pmatrix} 0 & 0 & 0 \\ 1 & 1 & 1 \\ 1 & 1 & 1 \end{pmatrix}, \\ \bar{u}_1^1 &= \begin{pmatrix} 1 & 1 & 0 \\ 1 & 1 & 1 \\ 1 & 1 & 1 \end{pmatrix}, & \bar{u}_1^2 &= \begin{pmatrix} 1 & 0 & 0 \\ 1 & 1 & 0 \\ 1 & 1 & 1 \end{pmatrix}, \\ \bar{u}_2^1 &= \begin{pmatrix} 1 & 0 & 0 \\ 1 & 1 & 1 \\ 1 & 1 & 1 \end{pmatrix}, & \bar{u}_2^2 &= \begin{pmatrix} 0 & 0 & 0 \\ 1 & 1 & 0 \\ 1 & 1 & 1 \end{pmatrix}. \end{aligned}$$

Further we use the following notations:

$$\begin{aligned} \tilde{\mathcal{U}} &= \{\bar{u}_0, \bar{u}_1^1, \bar{u}_1^2, \bar{u}_2^1, \bar{u}_2^2\}. \\ \mathcal{U} &= G\tilde{\mathcal{U}}. \end{aligned} \tag{9}$$

The  $p$ -contour  $\Omega_x$  is regular if it is composed by tiles of  $\mathcal{U}$ . Let  $\mathfrak{M}$  be the class of all the models satisfying the conditions **\Phi1** and **\Phi2**.

A model of  $\mathfrak{M}$  is called *regular* if for any configuration  $\mathbf{x}$  we have the following: if  $t, s \in \mathcal{A}_n$  belong to a connected component of  $\Omega_x$  then there exists a configuration  $\mathbf{y}$  such that one of the connected components of  $\Omega_y$  includes  $s$  and  $t$ , all tiles of this component belong to  $\mathcal{U}$  and  $H(\mathbf{y}) \leq H(\mathbf{x})$ .

Let  $\mathfrak{M}_r$  be the class of regular models.

We derive a classification of the macro-droplet shapes for the models of this class. In order to formulate the corresponding theorem we introduce the following notations:

$$\begin{aligned} E_0 &= 2\Phi \begin{pmatrix} 0 & 0 & 0 \\ 1 & 1 & 1 \\ 1 & 1 & 1 \end{pmatrix}, \\ E_{1/2} &= \Phi \begin{pmatrix} 0 & 1 & 1 \\ 1 & 1 & 1 \\ 1 & 1 & 1 \end{pmatrix} + \Phi \begin{pmatrix} 0 & 0 & 0 \\ 0 & 1 & 1 \\ 1 & 1 & 1 \end{pmatrix} + \Phi \begin{pmatrix} 0 & 0 & 0 \\ 0 & 0 & 0 \\ 0 & 1 & 1 \end{pmatrix}, \\ E_1 &= 2 \left( \Phi \begin{pmatrix} 0 & 1 & 1 \\ 1 & 1 & 1 \\ 1 & 1 & 1 \end{pmatrix} + \Phi \begin{pmatrix} 0 & 0 & 1 \\ 0 & 1 & 1 \\ 1 & 1 & 1 \end{pmatrix} \right), \end{aligned} \tag{10}$$



and

$$e_{1/2} = \frac{E_{1/2}}{E_0}, \quad e_1 = \frac{E_1}{E_0}. \quad (11)$$

The meaning of the subscripts will be cleared later.

It follows from **\Phi 2** that  $E_0 > 0$ ,  $E_{1/2} > 0$  and  $E_1 > 0$ . This can be easily proved by considering configurations  $\mathbf{y}_0$ ,  $\mathbf{y}_{1/2}$  and  $\mathbf{y}_1$  on a big rectangular volume as follows. For large  $n$  consider functions  $g_0^i$ ,  $g_{1/2}^i$ ,  $g_1^i$ ,  $i = 1, 2$ , defined on  $[-1, 1]$ :

$$\frac{dg_\varepsilon^i}{dt} = -\varepsilon, \quad g_\varepsilon^1(0) = \frac{m}{n}, \quad g_\varepsilon^2(0) = -\frac{m}{n}, \quad (12)$$

where  $\varepsilon \in \{0, \frac{1}{2}, 1\}$  and  $m$  is a fixed integer greater than 5. Consider the configurations  $\mathbf{y}_\varepsilon$  on  $\frac{1}{n}\mathbb{Z}^2$  defined by:

$$\mathbf{y}_\varepsilon(t) = \begin{cases} 0, & \text{if } t = (t_1, t_2) \in A_n \text{ and } g_\varepsilon^1(t_1) \leq t_2 \leq g_\varepsilon^2(t_1), \\ 1, & \text{otherwise.} \end{cases} \quad (13)$$

Because of **\Phi 2** every  $\mathbf{y}_\varepsilon$  has a positive energy. It is easy to check that if  $n$  is large then  $4nE_\varepsilon$  gives the main contribution to the energy of  $\mathbf{y}_\varepsilon$  and therefore  $E_\varepsilon > 0$ .

The subscript in  $E_\varepsilon$  and  $e_\varepsilon$  means that the derivative of the functions in Eq. (12) is  $-\varepsilon$  and that the corresponding configurations defined in Eq. (13) have the main contribution to energy given by  $E_\varepsilon$ .

We part  $\mathfrak{M}_r$  in the following regions defined by the values of  $e_{1/2}$ ,  $e_1$ :

$$\begin{aligned} A_{17} &= \{(e_{1/2}, e_1) : e_{1/2} \geq \frac{3}{2}, e_1 \geq 2\}, \\ A_{15} &= \{(e_{1/2}, e_1) : e_1 \leq 2e_{1/2} - 1, 1 \leq e_1 \leq 2\}, \\ A_{45} &= \{(e_{1/2}, e_1) : e_1 \leq e_{1/2}, e_1 \leq 1\}, \\ A_{13} &= \{(e_{1/2}, e_1) : e_1 \geq 2e_{1/2} - 1, 1 \leq e_{1/2} \leq \frac{3}{2}\}, \\ A_{23} &= \{(e_{1/2}, e_1) : e_1 \geq e_{1/2}, e_{1/2} \leq 1\}, \\ A_{35} &= \{(e_{1/2}, e_1) : e_1 \leq \frac{4}{3}e_{1/2}, e_1 \geq e_{1/2}, e_1 \geq 2e_{1/2} - 1\}, \\ A_{36} &= \{(e_{1/2}, e_1) : e_1 \geq \frac{4}{3}e_{1/2}, e_{1/2} \leq \frac{3}{2}\}. \end{aligned} \quad (14)$$

Every region  $A_{ij}$  includes all models of  $\mathfrak{M}_r$  having the values  $(e_{1/2}, e_1)$  in the corresponding domain.

We describe the macro-droplet shapes by determining their boundaries in the domain  $\{(\lambda_1, \lambda_2) : \lambda_2 \geq \lambda_1 \geq 0\}$ . The boundaries are defined as a function  $d$  having its graph stretched between the axis  $\lambda_1 = 0$  and the

diagonal  $\lambda_1 = \lambda_2$ . We consider the droplets with an area equal to 1. Therefore, the portion of the droplet area in the pointed domain is equal to  $\frac{1}{8}$ . The coefficients  $\delta$  in the theorem below must be chosen such that the droplet area is equal to 1. Of course, those coefficients may easily be computed. However, not to overload the formulae for  $d$  we left them non-computed. It is clear that  $\delta$  takes different values in the different areas, however we do not use subscripts to lighten notations.

**Theorem 2.** For the models of  $\mathfrak{M}$ , the macro-droplet shapes are as follows:

1. in  $A_{17}$

$$d(\lambda_1) = 2\delta, \quad \text{if } \lambda_1 \in [0, 2\delta] \quad (15)$$

2. in  $A_{45}$

$$d(\lambda_1) = -\lambda_1 + 2\delta, \quad \text{if } \lambda_1 \in [0, \delta e_1]. \quad (16)$$

3. in  $A_{15}$

$$d(\lambda_1) = \begin{cases} 2\delta, & \text{if } \lambda_1 \in [0, 2\delta(e_1 - 1)], \\ -\lambda_1 + 2\delta e_1, & \text{if } \lambda_1 \in [2\delta(e_1 - 1), \delta e_1], \end{cases} \quad (17)$$

4. in  $A_{13} \cap A_{35}$

$$d(\lambda_1) = \begin{cases} 2\delta, & \text{if } \lambda_1 \in [0, 4\delta(e_{1/2} - 1)], \\ -\frac{1}{2}\lambda_1 + 2\delta e_{1/2}, & \text{if } \lambda_1 \in [4\delta(e_{1/2} - 1), 4\delta(e_1 - e_{1/2})], \\ -\lambda_1 + 2\delta e_1, & \text{if } \lambda_1 \in [4\delta(e_1 - e_{1/2}), \delta e_1]. \end{cases} \quad (18)$$

5. in  $A_{13} \cap A_{36}$

$$d(\lambda_1) = \begin{cases} 2\delta, & \text{if } \lambda_1 \in [0, 4\delta(e_{1/2} - 1)], \\ -\frac{1}{3}\lambda_1 + 2\delta e_{1/2}, & \text{if } \lambda_1 \in [4\delta(e_{1/2} - 1), \frac{4}{3}\delta e_{1/2}], \end{cases} \quad (19)$$

6. in  $A_{23} \cap A_{36}$

$$d(\lambda_1) = -\frac{1}{2}\lambda + 2\delta, \quad \text{if } \lambda \in [0, \frac{4}{3}\delta], \quad (20)$$

7. in  $A_{23} \cap A_{35}$

$$d(\lambda_1) = \begin{cases} -\frac{1}{2}\lambda_1 + 2\delta e_{1/2}, & \text{if } \lambda_1 \in [0, 4\delta(e_1 - e_{1/2})], \\ -\lambda_1 + 2\delta e_1, & \text{if } \lambda_1 \in [4\delta(e_1 - e_{1/2}), \delta e_1], \end{cases} \quad (21)$$

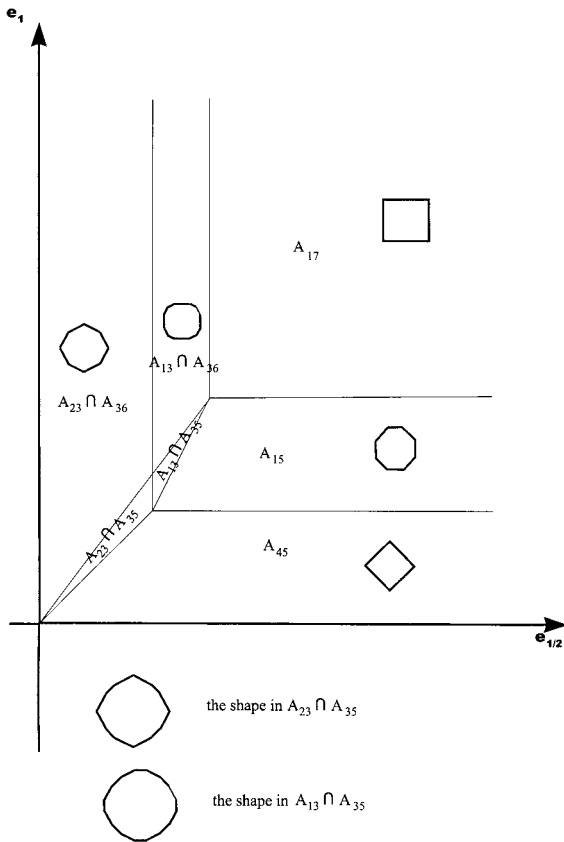


Fig. 1. Regions and associated polygons.

The result is illustrated on Fig. 1, where the macro-droplet shapes are shown for the regions  $A_{ij}$ .

The subscripts in the region notations come from the linear programming problem we solve to find the macro-droplet shape. There are seven coefficients and two relations between the coefficients in the problem. Every coefficient corresponds to a slope of a straight line defining the macro-droplet shape. The two integers of a region notation subscript refer to the slopes from which the macro-droplet boundary is built.

Observe that in  $A_{17}$ ,  $A_{45}$  and  $A_{23} \cap A_{36}$  the polygons do not depend on their boundary energy. We call those polygons *pure* one. In other regions the polygon shape is a function of the energy. They can be considered as a mixture of pure polygons.

A familiar shape of a macro-droplet is presented in  $A_{17}$ . The co-ordinates of the Ising model in the plane  $(e_{1/2}, e_1)$  is  $(\frac{3}{2}, 2)$ .

We introduce a class of models determined as follows:

1.  $\Phi(\bar{v}_0) = \Phi(\bar{v}_1) = 0$ ;
2.  $\min_{\bar{u} \in \mathcal{U}} \Phi(\bar{u}) > 0$ ;
3.  $\max_{\bar{u} \in \mathcal{U}} \Phi(\bar{u}) < \min_{\substack{\bar{w} \notin \mathcal{U} \\ \bar{w} \neq \bar{v}_0 \text{ and } \bar{v}_1}} \Phi(\bar{w})$ .

These models belong to  $\mathfrak{M}_r$ . Intuitively this is clear since any tile in the micro-droplet contour which do not belong to  $\mathcal{U}$  can be “substituted” by tiles from  $\mathcal{U}$  which decreases the energy. The set of all of these models covers the plane  $(e_{1/2}, e_1)$ . The most interesting of these models are those for which the value of  $(e_{1/2}, e_1)$  lies within the region  $A_{13} \cap A_{35}$ , where the droplets are 16-edges polygons. Particularly, a model for which  $(e_{1/2}, e_1) = (\frac{\sqrt{5}}{2}, \sqrt{2})$  and referred to *chien model* was introduced in ref. 10 and used in image processing applications (see refs. 11 and 12).

### 3. PROOF

#### 3.1. The Surface Tension

Our approach is based on the Wulff construction. The main step is the computation of the surface tension (see ref. 4). In these calculations we do not use the scaling by  $\frac{1}{n}$ .

For  $\sigma \in \mathbb{R}$ , we define a boundary condition out of  $V_N = \{t = (t_1, t_2) \in \mathbb{Z}^2 : |t_i| \leq N, i = 1, 2\}$  as follows:

$$\mathbf{x}_\sigma(t) = \begin{cases} 1, & \text{if } \sigma t_1 + t_2 \geq 0 \\ 0, & \text{if } \sigma t_1 + t_2 < 0. \end{cases} \quad (22)$$

Let  $\mathbf{X}_V(\sigma) = X^V \times \{\mathbf{x}_\sigma\}$  be the set of configurations obtained by joining every configuration of  $X^V$  with  $\mathbf{x}_\sigma$ . We use  $V$  to denote  $V_N$  when the value  $N$  is fixed or not important. Let  $Z(V, \beta, \sigma) = \sum_{\mathbf{x} \in \mathbf{X}_V(\sigma)} \exp\{-\beta H(\mathbf{x})\}$  be the partition function in the volume  $V$  given the boundary condition (22) at temperature  $T = \frac{1}{\beta}$ . Let  $Z(V, \beta)$  be the partition function in  $V$  given the boundary condition equal to 1 on  $V^c$ .

The surface tension along the slope defined by  $\sigma$  at zero temperature is given by:

$$\tau_\sigma = -\lim_{N \rightarrow \infty} \lim_{\beta \rightarrow \infty} \frac{1}{\beta d_{\sigma, N}} \log \frac{Z(V, \beta, \sigma)}{Z(V, \beta)}, \tag{23}$$

where  $d_{\sigma, N} = 2N \sqrt{1 + \sigma^2}$  is the distance between the points  $(-N, \sigma N)$  and  $(N, -\sigma N)$ .

Remark that the interior limit in (23) drastically simplifies the computations of  $\tau_\sigma$  with respect to the case of a finite temperature (see ref. 4). It is easy to see that for  $\beta \rightarrow \infty$

$$\frac{1}{\beta d_{\sigma, N}} \log \frac{Z(V, \beta, \sigma)}{Z(V, \beta)} = \frac{H_\sigma^*}{d_{\sigma, N}} + O\left(\frac{1}{\beta}\right), \tag{24}$$

where  $H_\sigma^* = \min_{\mathbf{x} \in X_V(\sigma)} H(\mathbf{x})$ . Hence it is enough to find  $x_\sigma^*$  such that  $H(x_\sigma^*) = H_\sigma^*$  for each slope  $\sigma$ .

Because of the symmetry properties of the potentials it is enough to compute the surface tensions for  $\sigma \in [0, 1]$ .

Besides  $p$ -contours, we use the standard notion of a *contour* of configurations. Let  $\mathbf{x} \in X_V(\sigma)$  then a set of bonds  $\mathcal{E}_x$  is a contour of  $\mathbf{x}$  if  $\mathbf{x}(t^1) \neq \mathbf{x}(t^2)$  for every  $b = \langle t^1, t^2 \rangle \in \mathcal{E}_x$ . We also use the notion of dual lattice  $\mathbb{Z}_*^2 = \mathbb{Z}^2 + (\frac{1}{2}, \frac{1}{2})$ . For any vertical (horizontal) bond  $b = \langle t^1, t^2 \rangle$ , where  $t^1 + (0, 1) = t^2$  ( $t^1 + (1, 0) = t^2$ ) there exists a horizontal (vertical) dual bond  $b^* = \langle t_*^1, t_*^2 \rangle$  of the dual lattice  $\mathbb{Z}_*^2$  intersecting  $b$ ; that is  $t_*^1 = t^1 + (\frac{1}{2}, \frac{1}{2})$  and  $t_*^2 = t^2 - (\frac{1}{2}, \frac{1}{2})$ . Then  $t_*^1 - (0, 1) = t_*^2$  ( $t_*^1 - (1, 0) = t_*^2$ ).

The contour of  $\mathbf{x} \in X_V(\sigma)$  in term of  $\mathbb{Z}_*^2$  is the set  $\mathcal{E}_x^*$  of all bonds dual to bonds from  $\mathcal{E}_x$ . The set  $\mathcal{E}_x^*$  can be split in maximal connected components. All components except one are closed lines. The exception is a non-closed line  $\Gamma_x^*$  which connects the bond  $b^{* \text{ in}}$  to  $b^{* \text{ out}}$ , where:

$$\begin{aligned} b^{* \text{ in}} &= \langle (-N - \frac{3}{2}, \varphi^- - \frac{1}{2}), (-N - \frac{1}{2}, \varphi^- - \frac{1}{2}) \rangle, \\ b^{* \text{ out}} &= \langle (N + \frac{1}{2}, \varphi^+ - \frac{1}{2}), (N + \frac{3}{2}, \varphi^+ - \frac{1}{2}) \rangle, \end{aligned} \tag{25}$$

with  $\varphi^- = \inf\{\varphi \in \mathbb{Z} : \varphi \geq \sigma(N + 1)\}$ ,  $\varphi^+ = \sup\{\varphi \in \mathbb{Z} : \varphi \geq -\sigma(N + 1)\}$ .

The set  $\Gamma_x$  of bonds in  $\mathbb{Z}^2$  is dual to  $\Gamma_x^*$ . If  $b = \langle t^1, t^2 \rangle$  then we note  $\{b\} = \{t_1, t_2\}$ . Let  $\{\Gamma_x\} = \bigcup_{b \in \Gamma_x} \{b\}$ . The same notations are used for the dual objects  $b^* \in \Gamma_x^* : \{b^*\}$  and  $\{\Gamma_x^*\}$ .

We call the set of bonds  $\Gamma_x$  the *splitting contour*. We consider the splitting contour as a directed set of bonds. The direction of  $\Gamma_x$  is defined by choosing a direction in  $\Gamma_x^*$ . First we choose the direction in  $\{\Gamma_x^*\}$  from the point  $(-N - \frac{3}{2}, \varphi^- - \frac{1}{2}) \in \{\Gamma_x^*\}$  to  $(N + \frac{3}{2}, \varphi^+ - \frac{1}{2}) \in \{\Gamma_x^*\}$ . Namely a point

$t_1^* \in \{\Gamma_x^*\}$  is less than  $t_2^* \in \{\Gamma_x^*, t_1^* < t_2^*\}$ , if the unique way along  $\{\Gamma_x^*\}$  connecting  $t_1^*$  to  $(-N - \frac{3}{2}, \varphi^- - \frac{1}{2})$  does not include  $t_2^*$ . Then the direction in  $\Gamma_x^*$  corresponding to the direction on  $\{\Gamma_x^*\}$  is defined as follows: a bond  $b_1^* \in \Gamma_x^*$  is less than  $b_2^* \in \Gamma_x^*$ ,  $b_1^* < b_2^*$ , if any site of  $\{b_1^*\}$  is not greater than every site of  $\{b_2^*\}$ . Next, a bond  $b_1 \in \Gamma_x$  is less than  $b_2 \in \Gamma_x$ ,  $b_1 < b_2$ , if the same relation  $b_1^* < b_2^*$  holds for the dual bonds. Let  $\hat{\Gamma}_x$  be a set of sites such that  $t \in \hat{\Gamma}_x$  if there exists  $b \in \Gamma_x$  such that  $b \subset W_t$ . Recall that  $W_t = \{u \in \mathbb{Z}^2 : |t - u| \leq \sqrt{2}\}$ . Apparently that  $\{\Gamma_x\} \subset \hat{\Gamma}_x$ .

Let  $g$  be a continuous function on  $[-N - 1, N + 1]$  such that

$$N + 1 \geq g(-N - 1) \geq g(N + 1) \geq -N - 1. \quad (26)$$

Consider the following configuration on  $V_N$

$$\mathbf{x}_g(t_1, t_2) = \begin{cases} 1, & \text{if } t_2 \geq g(t_1), \\ 0, & \text{if } t_2 < g(t_1). \end{cases} \quad (27)$$

It is clear that  $\mathbf{x}_g \in \mathbf{X}_{V_N}(\sigma)$ , where  $\sigma = \frac{g(-N-1) - g(N+1)}{2N+2}$ . Any function  $g$  on  $[-N - 1, N + 1]$  with (26) is called a *splitting function*.

It follows from the regularity that for any configuration  $\mathbf{x} \in \mathbf{X}_{V_N}(\sigma)$  there exists a configuration  $\mathbf{y} \in \mathbf{X}_{V_N}(\sigma)$  such that the splitting contour  $\Gamma_y$  is regular and  $H(\mathbf{y}) \leq H(\mathbf{x}) + o(1)$ . At zero temperature any configuration of  $\mathbf{X}_{V_N}(\sigma)$  minimizing the energy has no contour except a splitting contour. Thus we can restrict our considerations only to the set of configurations with a regular splitting contour.

Therefore to study the surface tension we only consider configurations of  $\mathbf{X}_{V_N}(\sigma)$  with a regular contour.

Let

$$\varepsilon_N(\sigma) = \frac{H(\mathbf{x}_\sigma^*)}{2E_0N}, \quad (28)$$

where  $E_0$  is defined in (10) and  $\mathbf{x}_\sigma^* \in \mathbf{X}_V(\sigma)$  is a configuration having minimal energy. Our closest goal is to find the configurations  $\mathbf{x}_\sigma^*$  in  $V_N$  for large  $N$  and for  $\sigma \in [0, 1]$ . In fact we find a configuration  $\mathbf{x}_\sigma^* \in \mathbf{X}_{V_N}(\sigma)$  such that the energy of  $\mathbf{x}_\sigma^*$  is minimal in  $\mathbf{X}_{V_N}(\sigma)$  up to a constant which is independent from  $N$ .

The next proposition gives the value of  $\varepsilon(\sigma) = \lim_{N \rightarrow \infty} \varepsilon_N(\sigma)$  as a function of  $\sigma \in [0, 1]$  for the regular models.

**Proposition 3.** For the models in  $\mathfrak{M}$ , the minimal value of the energy is:

If  $\sigma \leq \frac{1}{2}$  then

$$\varepsilon(\sigma) = \begin{cases} 2e_{1/2}, & \text{if } (e_{1/2}, e_1) \in A_{23}, \\ 2e_1, & \text{if } (e_{1/2}, e_1) \in A_{45}, \\ 4(e_{1/2} - 1)\sigma + 2, & \text{if } (e_{1/2}, e_1) \in A_{13}, \\ 2(e_1 - 1)\sigma + 2, & \text{if } (e_{1/2}, e_1) \in A_{15}, \\ 2\sigma + 2, & \text{if } (e_{1/2}, e_1) \in A_{17}. \end{cases} \quad (29)$$

If  $\sigma > \frac{1}{2}$  then the energy  $\varepsilon(\sigma)$  has the same expressions as in the case  $\sigma \leq \frac{1}{2}$  if  $(e_{1/2}, e_1) \in A_{17} \cup A_{15} \cup A_{45}$ . For the other regions of  $(e_{1/2}, e_1)$  we have

$$\varepsilon(\sigma) = \begin{cases} 4(e_1 - e_{1/2})\sigma + 2(2e_{1/2} - e_1), & \text{if } (e_{1/2}, e_1) \in A_{35}, \\ \frac{4}{3}e_{1/2}\sigma + \frac{4}{3}e_{1/2}, & \text{if } (e_{1/2}, e_1) \in A_{36}. \end{cases} \quad (30)$$

Observe that  $\varepsilon(\sigma)$  is linear in  $A_{15}$ ,  $A_{17}$  and  $A_{45}$ , and piece-wise linear in  $A_{23} \cap A_{36}$ ,  $A_{13} \cap A_{36}$ ,  $A_{23} \cap A_{35}$  and  $A_{13} \cap A_{35}$ .

*Proof.* The proof is composed of two parts. In the first one we find  $\mathbf{y}_\sigma^*$  having minimal energy among configurations having a so called ‘‘canonical’’ splitting contour. In the second step we show that for a configuration  $\mathbf{x} \in \mathbf{X}_{V_N}(\sigma)$  with an arbitrary regular contour we can find a configuration  $\mathbf{y} \in \mathbf{X}_{V_N}(\sigma)$  having a ‘‘canonical’’ splitting contour and such that  $H(\mathbf{y}) \leq H(\mathbf{x})$ . The second step is rather technical and we locate it in Appendix.

**Step 1.** The Optimal Shape of Canonical Contours. We define the canonical splitting contour by a splitting function:

$$g(-N) = \sigma N, \quad \frac{d}{dt} g(s) = \begin{cases} -\sigma & \text{if } s \in (-N-1, -N) \\ 0 & \text{if } s \in (-N, s_0), \\ \frac{1}{2} & \text{if } s \in (s_0, s_{1/2}^+), \\ -\frac{1}{2} & \text{if } s \in (s_{1/2}^+, s_{1/2}^-), \\ 1 & \text{if } s \in (s_{1/2}^-, s_1^+), \\ -1 & \text{if } s \in (s_1^+, s_1^-), \\ -2 & \text{if } s \in (s_1^-, N), \\ -(g(N) - \sigma N) & \text{if } s \in (N, N+1), \end{cases} \quad (31)$$

where  $s_0 \leq s_{1/2}^+ \leq s_{1/2}^- \leq s_1^+ \leq s_1^-$  belong to the interval  $[-N, N]$  and are such that  $s_{1/2}^+ - \frac{1}{2}s_0 - \frac{3}{2}s_{1/2}^- + 2s_1^+ + s_1^- - 2N(1 - \sigma) \geq 0$  (see Fig. 2). There are 7 linear pieces which constitute the splitting function  $g$  of a canonical

splitting contour on  $[-N, N]$ . The derivatives of the pieces are  $0, \pm\frac{1}{2}, \pm 1, -2,$  and  $-(g(N) - \sigma N)$ . If  $g(N) > -\sigma N$  then the last linear piece of  $g$  creates a vertical interval of the dual lattice along which the corresponding configuration  $y_g$  takes different values on both sides. Next we find the splitting function such that the corresponding configuration has the minimal energy.

**Lemma 4.** Let  $Z_{V_N}(\sigma) \subseteq X_{V_N}(\sigma)$  be the set of configurations having a canonical splitting contour. Then the minimal energy for configurations of  $Z_{V_N}(\sigma)$  are the same as in Proposition 3.

*Proof.* We shall use the following notations

$$\begin{aligned} \alpha_1 &= s_0 + N, & \alpha_2 &= s_{1/2}^+ - s_0, & \alpha_3 &= s_{1/2}^- - s_{1/2}^+, \\ \alpha_4 &= s_1^+ - s_{1/2}^-, & \alpha_5 &= s_1^- - s_1^+, & \alpha_6 &= \frac{1}{\sigma} (g(s_1^-) - g(N)), \\ \alpha_7 &= \frac{1}{\sigma} (g(N) - \sigma N). \end{aligned}$$

The energy of the configuration  $x_g$  having  $g$  as a splitting function is

$$\mathcal{E} = E_0\alpha_1 + E_{1/2}(\alpha_2 + \alpha_3) + E_1(\alpha_4 + \alpha_5) + E_{1/2}\sigma\alpha_6 + E_0\sigma\alpha_7 + O(1), \quad (32)$$

as  $N \rightarrow \infty$ . The last term  $O(1)$  corresponds to the energy of the junctions between the pieces with different slopes. Our goal is to find a minimal value

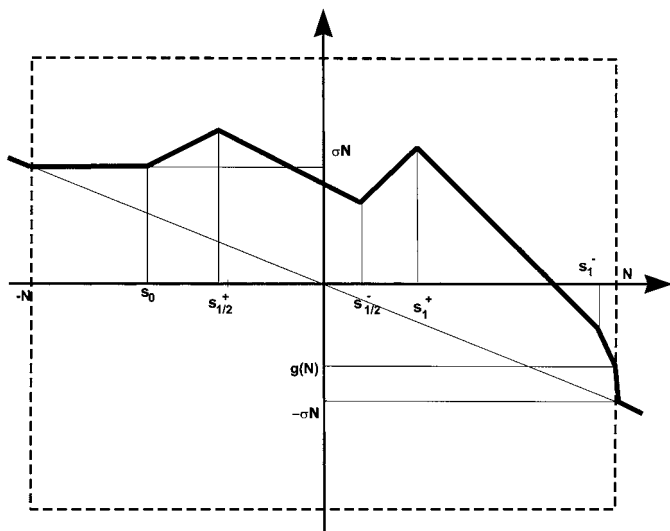


Fig. 2. Canonical contour.



of the energy in (32). It means we have to find values of the variables  $\alpha_i$  minimizing (32). This is a standard problem of the linear programming.

There are two relations for the variables  $\alpha_i$ :

$$\begin{aligned} 2N &= \alpha_1 + \alpha_2 + \alpha_3 + \alpha_4 + \alpha_5 + \frac{1}{2}\sigma\alpha_6, \\ 2N\sigma &= -\frac{1}{2}(\alpha_2 - \alpha_3) - \alpha_4 + \alpha_5 + \sigma(\alpha_6 + \alpha_7), \end{aligned} \quad (33)$$

that are an easy consequence of the splitting function definition.

We study separately the cases  $\sigma \leq \frac{1}{2}$  and  $\sigma > \frac{1}{2}$ .

Let  $\sigma \leq \frac{1}{2}$ . Using (33) we can exclude any pair  $(\alpha_i, \alpha_j)$ ,  $i \neq j$ , of variables in (32). We obtain the following expressions of the energy:

$$\begin{aligned} \mathcal{E}(\hat{\alpha}_2, \hat{\alpha}_3) &= \alpha_1(E_0 - E_{1/2}) + \alpha_4(E_1 - E_{1/2}) + \alpha_5(E_1 - E_{1/2}) + \sigma\alpha_6 \frac{1}{2}E_{1/2} \\ &\quad + \sigma\alpha_7 E_0 + 2NE_{1/2} + O(1), \\ \mathcal{E}(\hat{\alpha}_4, \hat{\alpha}_5) &= \alpha_1(E_0 - E_1) + (\alpha_2 + \alpha_3)(E_{1/2} - E_1) + \sigma\alpha_6(E_{1/2} - \frac{1}{2}E_1) + \sigma\alpha_7 E_0 \\ &\quad + 2NE_1 + O(1), \\ \mathcal{E}(\hat{\alpha}_1, \hat{\alpha}_3) &= \alpha_2 2(E_{1/2} - E_0) + \alpha_4(2E_{1/2} - 3E_0 + E_1) + \alpha_5(E_0 - 2E_{1/2} + E_1) \\ &\quad + \sigma\alpha_6(\frac{3}{2}E_0 - E_{1/2}) + \sigma\alpha_7(3E_0 - 2E_{1/2}) \\ &\quad + 2(1 - 2\sigma)NE_0 + 4\sigma NE_{1/2} + O(1), \\ \mathcal{E}(\hat{\alpha}_1, \hat{\alpha}_5) &= \alpha_2(E_{1/2} + \frac{1}{2}E_1 - \frac{3}{2}E_0) + \alpha_3(E_{1/2} - \frac{1}{2}E_1 - \frac{1}{2}E_0) + \alpha_4 2(E_1 - E_0) \\ &\quad + \sigma\alpha_6(\frac{1}{2}E_0 + E_{1/2} - E_1) + \sigma\alpha_7(2E_0 + E_1) \\ &\quad + 2(1 - \sigma)NE_0 + 2\sigma NE_1 + O(1), \\ \mathcal{E}(\hat{\alpha}_1, \hat{\alpha}_7) &= \alpha_2(E_{1/2} - \frac{1}{2}E_0) + \alpha_3(E_{1/2} - \frac{3}{2}E_0) + \alpha_4 E_1 + \sigma\alpha_5(E_1 - 2E_0) \\ &\quad + \sigma\alpha_5(E_{1/2} - \frac{3}{2}E_0) + 2(1 + \sigma)NE_0 + O(1), \end{aligned} \quad (34)$$

as  $N \rightarrow \infty$ . The symbol  $\mathcal{E}(\hat{\alpha}_i, \hat{\alpha}_j)$  means that the expression for the energy does not explicitly include the variables  $\alpha_i$  and  $\alpha_j$ . If the coefficients at the variables  $\alpha_i$  presented in a corresponding expression are positive then the minimal value of the energy is attained when the variables are equal to 0. For example, consider the first equality in (34). The positivity of all the coefficients at the variables  $\alpha_i$  defines a region in the space of the parameters  $e_{1/2}, e_1$ . It is the region  $A_{23}$  shown on the Fig. 1 (see (14)). In this region the minimal value of the energy is  $\mathcal{E}(\hat{\alpha}_2, \hat{\alpha}_3) = 2NE_{1/2} + O(1)$ . The

variables having non-zero values are  $\alpha_2 = N(1 - 2\sigma)$  and  $\alpha_3 = N(1 + 2\sigma)$ . The splitting function in this case is:

$$g(-N) = \sigma N, \quad \frac{d}{dt} g(s) = \begin{cases} \frac{1}{2} & \text{if } s \in (-N, 2 - 2\sigma N), \\ -\frac{1}{2} & \text{if } s \in (-2\sigma N, N). \end{cases} \quad (35)$$

A similar analysis can be performed for the 5 expressions given in (34). It is essential that the obtained results are valid only for  $\sigma \leq \frac{1}{2}$ . For example, we have a negative  $\alpha_2$  if  $\sigma > \frac{1}{2}$  in the first equation in (34). Let  $\sigma > \frac{1}{2}$ . It is not difficult to obtain that the answer is the same as in the previous case in the regions  $A_{17}$ ,  $A_{15}$  and  $A_{45}$ . To obtain optimal splitting lines and corresponding minimal energies in the regions  $A_{23}$  and  $A_{13}$  we use the following expressions for the energy

$$\begin{aligned} \mathcal{E}(\hat{\alpha}_3, \hat{\alpha}_5) &= \alpha_1(E_0 - 2E_{1/2} + E_1) + \alpha_2 2(E_1 - E_{1/2}) + \alpha_4 4(E_1 - E_{1/2}) \\ &\quad + \sigma \alpha_6 (2E_{1/2} - \frac{3}{2}E_1) + \sigma \alpha_7 (2E_{1/2} - 2E_1 + E_0) + 4N(1 - \sigma) E_{1/2} \\ &\quad + 2(2\sigma - 1) NE_1 + O(1) \end{aligned} \quad (36)$$

$$\begin{aligned} \mathcal{E}(\hat{\alpha}_3, \hat{\alpha}_6) &= \alpha_1(E_0 - \frac{2}{3}E_{1/2}) + \alpha_2 \frac{2}{3}E_{1/2} + \alpha_4 E_1 + \alpha_5 (E_1 - \frac{4}{3}E_{1/2}) \\ &\quad + \sigma \alpha_7 (E_0 - \frac{2}{3}E_{1/2}) + \frac{4}{3}(1 + \sigma) NE_{1/2} + O(1). \end{aligned}$$

For example, in  $A_{36}$  for  $\sigma > \frac{1}{2}$  we obtain

$$g(-N) = \sigma N, \quad \frac{d}{dt} g(s) = \begin{cases} -\frac{1}{2} & \text{if } s \in (-N, N(\frac{5}{3} - \frac{4}{3}\sigma)), \\ -2 & \text{if } s \in (N(\frac{5}{3} - \frac{4}{3}\sigma), N). \end{cases} \quad (37)$$

We have  $A_{13} \cup A_{23} = A_{35} \cup A_{36}$ . Hence the energy  $\varepsilon(\sigma)$  has two linear pieces as a function of  $\sigma$  in this region. ■

**Step 2.** In this step we study configurations with non-canonical splitting contours. Recall that we study regular models of  $\mathfrak{M}_r$ . Hence we can consider configurations of  $\mathbf{X}_V(\sigma)$  having regular contours.

**Lemma 5.** Let  $\mathbf{x} \in \mathbf{X}_V(\sigma)$  and  $\mathcal{E}_{\mathbf{x}} = \Gamma_{\mathbf{x}}$ . Then there exists a configuration  $\mathbf{x}_0 \in \mathbf{X}_V(\sigma)$  such that  $H(\mathbf{x}_0) \leq H(\mathbf{x})$ ,  $\mathcal{E}_{\mathbf{x}_0} = \Gamma_{\mathbf{x}_0}$  and  $\Gamma_{\mathbf{x}_0}$  is canonical.

The main steps of this lemma proof are the following. First we remove all folds of the contour such that the resulting contour is monotone. Then we permute the monotone contour to obtain a contour composed by pieces constituted by tiles of the same type. The resulting contour is close to a canonical one. The last reconstruction gives a configuration  $\mathbf{x}_0$  having a

canonical contour  $\Gamma_{x_0}$  with the same slope as  $\Gamma_x$ . The energy of the configuration  $x_0$  is not greater than the energy of  $x$ .

The complete proof is given in the Appendix.

### 3.2. Shape

As we have seen in the previous section the minimal energy  $\varepsilon(\sigma)$  is a piece-wise linear function of  $\sigma$ .

The surface tension  $\tau_\sigma$  is given by:

$$\tau_\sigma = \frac{\varepsilon(\sigma)}{\sqrt{1+\sigma^2}}, \tag{38}$$

(see (23), (24), and (28)). To find the droplet shapes we use the Wulff construction.<sup>(4)</sup> Let (see ref. 4, chap. 2, (2.1.2))

$$S_\sigma = \left\{ \lambda = (\lambda_1, \lambda_2) \in \mathbb{R}_+^2 : \frac{\lambda_1\sigma + \lambda_2}{\sqrt{1+\sigma^2}} \leq \frac{\varepsilon_N(\sigma)}{\sqrt{1+\sigma^2}} \right\}. \tag{39}$$

Let also  $T_0 = \{\lambda = (\lambda_1, \lambda_2) \in \mathbb{R}_+^2 : \lambda_1 \geq 0\}$  and  $T_1 = \{\lambda = (\lambda_1, \lambda_2) \in \mathbb{R}_+^2 : \lambda_2 - \lambda_1 \geq 0\}$ . Then the Wulff construction defines the droplet shape as follows:  $S = \bigcap_{\sigma \in [0, 1]} S_\sigma \cap T_0 \cap T_1$ . In fact  $S$  is one eighth of the droplet. The whole droplet can be obtained by the reflections of  $S$  with respect to the diagonals and the axes.

Let  $\varepsilon(\sigma) = a\sigma + b$  be a linear function, where  $0 \leq a \leq b$ . Then the point  $(a, b) \in \mathbb{R}^2$  belongs to the boundaries of all  $S_\sigma$ . Hence  $S = S_0 \cap S_1 \cap T_0 \cap T_1$ . The boundary  $d(\lambda)$  of the droplet in the domain  $\{\lambda = (\lambda_1, \lambda_2) \in \mathbb{R}^2 : 0 \leq \lambda_1 \leq \lambda_2\}$  is given by:

$$d(\lambda) = \begin{cases} b, & \text{if } \lambda \in [0, a] \\ -\lambda + a + b, & \text{if } \lambda \in [a, \frac{a+b}{2}] \end{cases} \tag{40}$$

If  $a = b$  then  $S = S_0 \cap T_0 \cap T_1$  and if  $a = 0$  then  $S = S_1$ . In the considered cases we have  $a = b$  in the region  $A_{17}$  since  $\varepsilon(\sigma) = 2\sigma + 2$ . Therefore the droplet boundary  $d$  is the horizontal straight line. The case  $a = 0$  holds in the region  $A_{45}$ , where  $\varepsilon(\sigma) = 2e_1$ . Hence  $d$  is a straight line with its slope  $-1$ . In the region  $A_{15}$  the droplet boundary is like in (40) with  $a = 2(e_1 - 1)$  and  $b = 2$ . Recall that  $1 \leq e_1 \leq 2$  in  $A_{15}$ .

In the region  $A_{23} \cup A_{13} = A_{36} \cup A_{35}$  the energy is a piece-wise linear function composed by two pieces. To find the droplet shape in the regions we shall use

**Lemma 6.** Let points  $(a_1, b_1)$  and  $(a_2, b_2)$  be such that  $a_1 + 2b_1 = a_2 + 2b_2$  and let

$$\varepsilon(\sigma) = \begin{cases} a_1\sigma + b_1, & \text{if } 0 \leq \sigma \leq \frac{1}{2}, \\ a_2\sigma + b_2, & \text{if } \frac{1}{2} \leq \sigma \leq 1. \end{cases}$$

Then

$$S = S_0 \cap S_{1/2} \cap S_1 \cap T_0 \cap T_1.$$

If  $a_1 \leq a_2$  then

$$d(\lambda) = \begin{cases} b_1, & \text{if } 0 \leq \lambda \leq a_1, \\ -\frac{1}{2}\lambda + (b_1 + \frac{1}{2}a_1), & \text{if } a_1 \leq \lambda \leq a_2, \\ -\lambda + (b_2 + a_2), & \text{if } a_2 \leq \lambda \leq \frac{a_2 + b_2}{2}, \end{cases} \quad (41)$$

if  $a_1 > a_2$  then

$$d(\lambda) = \begin{cases} b_1, & \text{if } 0 \leq \lambda \leq a_2 + b_2 - b_1, \\ -\lambda + (b_2 + a_2), & \text{if } a_2 + b_2 - b_1 \leq \lambda \leq \frac{a_2 + b_2}{2}, \end{cases} \quad (42)$$

Remark that since  $a_1 + 2b_1 = a_2 + 2b_2$  we have that  $\frac{1}{2}(a_2 + b_2) \leq b_1$ . Therefore the interval  $[a_2 + b_2 - b_1, \frac{1}{2}(a_2 + b_2)]$  is not empty.

The proof is straightforward and omitted here.

We apply this lemma for the region  $B = A_{23} \cup A_{13}$ . There are four regions in  $B$  having different shapes of droplets. In the region  $A_{13} \cap A_{35}$  we have

$$\varepsilon(\sigma) = \begin{cases} 4(e_{1/2} - 1)\sigma + 2, & \text{if } 0 \leq \sigma \leq \frac{1}{2}, \\ 4(e_1 - e_{1/2})\sigma + 2(2e_{1/2} - e_1), & \text{if } \frac{1}{2} \leq \sigma \leq 1. \end{cases} \quad (43)$$

Hence  $a_1 = 4(e_{1/2} - 1)$ ,  $b_1 = 2$  and  $a_2 = 4(e_1 - e_{1/2})$ ,  $b_2 = 2(2e_{1/2} - e_1)$ . Recall that  $e_1 \geq 2e_{1/2} - 1$  in  $A_{13}$ . Thus  $a_1 \leq a_2$ . Using Lemma 6 we obtain in  $A_{13} \cap A_{35}$

$$d(\lambda) = \begin{cases} 2, & \text{if } \lambda \in [0, 4(e_{1/2} - 1)], \\ -\frac{1}{2}\lambda + 2e_{1/2}, & \text{if } \lambda \in [4(e_{1/2} - 1), 4(e_1 - e_{1/2})], \\ -\lambda + 2e_1, & \text{if } \lambda \in [4(e_1 - e_{1/2}), e_1]. \end{cases} \quad (44)$$

Similar considerations give the droplet shape in the last three subregions of  $B$ . The full result is formulated in Theorem 2.

We note that for all the subregions we have  $a_1 \leq a_2$ . However, some lines in (41) are trivial. The last line is trivial in  $A_{13} \cap A_{36}$  and  $A_{23} \cap A_{36}$ . Moreover the first line is trivial in  $A_{23} \cap A_{36}$ .

### 4. ON REGULARITY

In this section we give several examples of models such that the behaviour of the droplet micro-boundaries is dramatically different of that for the regular one. We discuss also sufficient conditions for regularity without giving proofs.

#### 4.1. Examples

The regularity requirement we used is essential for the proof of the main theorem. The next examples show that there exist models satisfying  $\Phi 1$  and  $\Phi 2$  with non-regular microdroplet boundaries.

In all the following examples, when we assign an energy value to a tile, we assume that all the tiles obtained from the first one by symmetrical transformations have the same energy.

**Example 1.** Let  $0 < a < b$ . As usually

$$\Phi(\bar{v}_0) = 0.$$

Let

$$\Phi \begin{pmatrix} 1 & 1 & 1 \\ 0 & 1 & 0 \\ 0 & 0 & 0 \end{pmatrix} = \Phi \begin{pmatrix} 1 & 1 & 1 \\ 1 & 1 & 1 \\ 0 & 1 & 0 \end{pmatrix} = \Phi \begin{pmatrix} 1 & 1 & 1 \\ 1 & 1 & 1 \\ 1 & 0 & 1 \end{pmatrix} = a.$$

All other tiles have energy equal to  $b$ . It is easy to understand that for large  $\frac{b}{a}$  the square composed of 0's with boundary as shown below has the minimal energy of all possible shapes.

```

1 1 1 1 1 1 1 1 1 1 1 1 1 1 1 1 1 1 1 1 1 1
0 1 0 1 0 1 0 1 0 1 0 1 0 1 0 1 0 1 0 1 0 1
0 0 0 0 0 0 0 0 0 0 0 0 0 0 0 0 0 0 0 0 0 0
0 0 0 0 0 0 0 0 0 0 0 0 0 0 0 0 0 0 0 0 0 0
    
```

**Example 2.** Let  $c > b > a > 0$ . The potential function is

$$(1) \quad \Phi(\bar{v}_0) = 0,$$

$$(2) \quad \Phi\left(\begin{pmatrix} 1 & 1 & 1 \\ 1 & 0 & 1 \\ 1 & 0 & 1 \end{pmatrix}\right) = \Phi\left(\begin{pmatrix} 1 & 1 & 1 \\ 0 & 1 & 0 \\ 0 & 1 & 0 \end{pmatrix}\right) = -a$$

$$(3) \quad \Phi\left(\begin{pmatrix} 1 & 1 & 1 \\ 1 & 1 & 1 \\ 0 & 1 & 0 \end{pmatrix}\right) = \Phi\left(\begin{pmatrix} 1 & 1 & 1 \\ 1 & 1 & 1 \\ 1 & 0 & 1 \end{pmatrix}\right) = b$$

$$(4) \quad \Phi(\bar{u}) = c \text{ for all tiles } \bar{u} \text{ not listed above.}$$

For large  $\frac{c}{b}$  the micro-droplet boundary looks like it is shown below

```

1 1 1 1 1 1 1 1 1 1 1 1 1 1 1 1 1 1 1 1 1 1 1 1 1 1 1 1 1 1 1 1 1
1 1 1 1 1 1 1 1 1 1 1 1 1 1 1 1 1 1 1 1 1 1 1 1 1 1 1 1 1 1 1 1 1
0 1 0 1 0 1 0 1 0 1 0 1 0 1 0 1 0 1 0 1 0 1 0 1 0 1 0 1 0 1 0 1 0
0 1 0 1 0 1 0 1 0 1 0 1 0 1 0 1 0 1 0 1 0 1 0 1 0 1 0 1 0 1 0 1 0
0 0 0 0 0 0 0 0 0 0 0 0 0 0 0 0 0 0 0 0 0 0 0 0 0 0 0 0 0 0 0 0 0
0 0 0 0 0 0 0 0 0 0 0 0 0 0 0 0 0 0 0 0 0 0 0 0 0 0 0 0 0 0 0 0 0

```

The conditions **Φ1** and **Φ2** hold since  $b > a$ .

Remark that we must have a negative value of the potential function for some tiles. If the energy value of the tiles listed in (2) is positive then the energy of the boundary in the picture above is not minimal.

We can not directly continue this idea for new examples having non-regular boundaries. It seems there is no model having droplet micro-boundary like shown below and satisfying **Φ2**:

```

1 1 1 1 1 1 1 1 1 1 1 1 1 1 1 1 1 1 1 1 1 1 1 1 1 1 1 1 1 1 1 1 1
1 1 1 1 1 1 1 1 1 1 1 1 1 1 1 1 1 1 1 1 1 1 1 1 1 1 1 1 1 1 1 1 1
0 1 0 1 0 1 0 1 0 1 0 1 0 1 0 1 0 1 0 1 0 1 0 1 0 1 0 1 0 1 0 1 0
0 1 0 1 0 1 0 1 0 1 0 1 0 1 0 1 0 1 0 1 0 1 0 1 0 1 0 1 0 1 0 1 0
0 1 0 1 0 1 0 1 0 1 0 1 0 1 0 1 0 1 0 1 0 1 0 1 0 1 0 1 0 1 0 1 0
0 0 0 0 0 0 0 0 0 0 0 0 0 0 0 0 0 0 0 0 0 0 0 0 0 0 0 0 0 0 0 0 0
0 0 0 0 0 0 0 0 0 0 0 0 0 0 0 0 0 0 0 0 0 0 0 0 0 0 0 0 0 0 0 0 0

```

However more sophisticated examples can be found.

**Example 3.** Let  $a > 0$  and  $c > b > 0$  be such that

$$8b > a \tag{45}$$

and  $c$  is large enough. We consider a model with

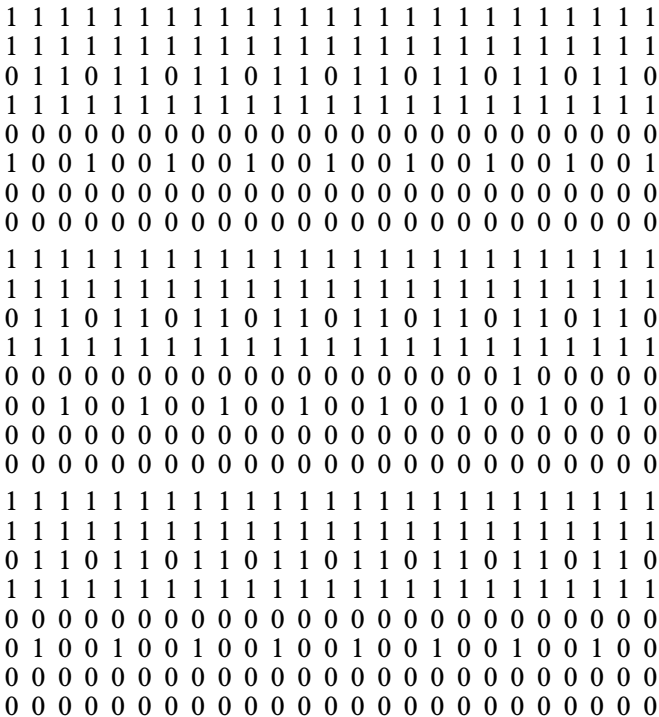
(1)  $\Phi(\bar{v}_0) = 0,$

(2)  $\Phi \begin{pmatrix} 1 & 1 & 1 \\ 1 & 0 & 1 \\ 1 & 0 & 1 \end{pmatrix} = -a$

(3)  $\Phi \begin{pmatrix} 1 & 1 & 1 \\ 1 & 1 & 1 \\ 0 & 1 & 0 \end{pmatrix} = \Phi \begin{pmatrix} 1 & 1 & 1 \\ 1 & 1 & 0 \end{pmatrix} = \Phi \begin{pmatrix} 0 & 0 & 0 \\ 1 & 1 & 1 \\ 1 & 1 & 0 \end{pmatrix} = \Phi \begin{pmatrix} 0 & 0 & 0 \\ 1 & 1 & 1 \\ 1 & 0 & 1 \end{pmatrix} = b$

(4) for all other tiles  $\bar{u}$  not listed above  $\Phi(\bar{u}) = c.$

The relation (45) gives  $\Phi 2$ . Then the boundary has one of the forms shown below.



There is a freedom in the boundary construction.

**Example 4.** Let  $\Phi$  is equal to  $a > 0$  for the following tiles

$$\begin{pmatrix} 1 & 1 & 1 \\ 1 & 1 & 1 \\ 0 & 1 & 1 \end{pmatrix}, \begin{pmatrix} 1 & 1 & 1 \\ 1 & 1 & 1 \\ 0 & 0 & 1 \end{pmatrix}, \begin{pmatrix} 1 & 1 & 1 \\ 0 & 0 & 1 \\ 1 & 1 & 0 \end{pmatrix}, \begin{pmatrix} 1 & 1 & 1 \\ 0 & 1 & 1 \\ 1 & 0 & 0 \end{pmatrix}, \begin{pmatrix} 0 & 0 & 1 \\ 1 & 1 & 0 \\ 0 & 0 & 1 \end{pmatrix}, \begin{pmatrix} 0 & 0 & 1 \\ 1 & 0 & 0 \\ 1 & 0 & 0 \end{pmatrix}.$$

All other tiles have an energy value equal to  $b > a$  except as usually the tiles  $\bar{v}_0, \bar{v}_1$  having the energy 0. If  $\frac{b}{a}$  is large then the droplet boundary is as shown in the following picture.

```

0 1 1 1 1 1 1 1 1 1 1 1 1 1 1 1 1 1 1 1 1 1 1 1 1 1 1 1 1 1 1 1 1 1
1 0 0 1 1 1 1 1 1 1 1 1 1 1 1 1 1 1 1 1 1 1 1 1 1 1 1 1 1 1 1 1 1 1
0 1 1 0 0 1 1 1 1 1 1 1 1 1 1 1 1 1 1 1 1 1 1 1 1 1 1 1 1 1 1 1 1 1
0 0 0 1 1 0 0 1 1 1 1 1 1 1 1 1 1 1 1 1 1 1 1 1 1 1 1 1 1 1 1 1 1 1
0 0 0 0 0 1 1 0 0 1 1 1 1 1 1 1 1 1 1 1 1 1 1 1 1 1 1 1 1 1 1 1 1 1
1 1 0 0 0 0 0 1 1 0 0 1 1 1 1 1 1 1 1 1 1 1 1 1 1 1 1 1 1 1 1 1 1 1
0 0 1 1 0 0 0 0 0 1 1 0 0 1 1 1 1 1 1 1 1 1 1 1 1 1 1 1 1 1 1 1 1 1
0 0 0 0 1 1 0 0 0 0 0 1 1 0 0 1 1 1 1 1 1 1 1 1 1 1 1 1 1 1 1 1 1 1
0 0 0 0 0 0 1 1 0 0 0 0 0 1 1 0 0 1 1 1 1 1 1 1 1 1 1 1 1 1 1 1 1 1
0 0 0 0 0 0 0 1 1 0 0 0 0 0 1 1 0 0 1 1 1 1 1 1 1 1 1 1 1 1 1 1 1 1
0 0 0 0 0 0 0 0 1 1 0 0 0 0 0 1 1 0 0 1 1 1 1 1 1 1 1 1 1 1 1 1 1 1
0 0 0 0 0 0 0 0 0 1 1 0 0 0 0 0 1 1 0 0 0 0 1 1 1 1 1 1 1 1 1 1 1 1
0 0 0 0 0 0 0 0 0 0 1 1 0 0 0 0 0 1 1 0 0 0 0 1 1 1 1 1 1 1 1 1 1 1
0 0 0 0 0 0 0 0 0 0 0 0 1 1 0 0 0 0 0 1 1 0 0 0 1 1 1 1 1 1 1 1 1 1
0 0 0 0 0 0 0 0 0 0 0 0 0 0 0 1 1 0 0 0 0 0 0 1 1 0 0 0 1 1 1 1 1 1
0 0 0 0 0 0 0 0 0 0 0 0 0 0 0 0 0 0 0 0 0 0 0 0 1 1 0 0 0 1 1 1 1 1
0 0 0 0 0 0 0 0 0 0 0 0 0 0 0 0 0 0 0 0 0 0 0 0 0 1 1 0 0 0 1 1 1 1
0 0 0 0 0 0 0 0 0 0 0 0 0 0 0 0 0 0 0 0 0 0 0 0 0 0 1 1 0 0 0 1 1 1
0 0 0 0 0 0 0 0 0 0 0 0 0 0 0 0 0 0 0 0 0 0 0 0 0 0 0 1 1 0 0 1 1 1
0 0 0 0 0 0 0 0 0 0 0 0 0 0 0 0 0 0 0 0 0 0 0 0 0 0 0 0 1 1 0 0 1 1
0 0 0 0 0 0 0 0 0 0 0 0 0 0 0 0 0 0 0 0 0 0 0 0 0 0 0 0 0 1 1 0 1 1
0 0 0 0 0 0 0 0 0 0 0 0 0 0 0 0 0 0 0 0 0 0 0 0 0 0 0 0 0 0 0 1 1 1

```

## 4.2. Conjectures About the Regularity

In this section we present two sufficient conditions of regularity. We assume that  $\Phi 1, \Phi 2$  are satisfied. It seems that both conditions cover a rather small area of models. We formulate them as theorems, however we do not prove them here. We think that the proof of the second theorem is not difficult. But a proof of the first one seems to be long and technical. Not to overload the text we do not give the proofs. One can consider these theorems as conjectures.

Both conditions are based on an energy prevailing assumption. The Ising model and some of the Gerzik–Dobrushin (see ref. 9) models satisfy the first condition and the chlen model (see ref. 10) satisfies the second one.



Let us consider the following set of tiles

$$\tilde{\mathcal{T}} = \left\{ \begin{pmatrix} 1 & 1 & 1 \\ 1 & 0 & 1 \\ r_{31} & r_{32} & r_{33} \end{pmatrix}, \begin{pmatrix} 1 & 1 & 0 \\ 1 & 0 & 1 \\ 1 & 0 & 1 \end{pmatrix}, \begin{pmatrix} 1 & 0 & 1 \\ 1 & 0 & 1 \\ 1 & 0 & 1 \end{pmatrix}, \begin{pmatrix} 1 & 1 & 0 \\ 1 & 0 & 1 \\ 1 & 0 & 0 \end{pmatrix}, \begin{pmatrix} 1 & 1 & 0 \\ 1 & 0 & 1 \\ 0 & 1 & 1 \end{pmatrix}, \right. \\ \left. \begin{pmatrix} 1 & 1 & 0 \\ 1 & 0 & 1 \\ 0 & 0 & 1 \end{pmatrix}, \begin{pmatrix} 1 & 1 & 0 \\ 0 & 0 & 0 \\ 1 & 1 & 1 \end{pmatrix}, \begin{pmatrix} 1 & 1 & 1 \\ 1 & 0 & 0 \\ 1 & 0 & 0 \end{pmatrix}, \begin{pmatrix} 1 & 1 & 1 \\ 1 & 0 & 0 \\ 0 & 0 & 1 \end{pmatrix} \right\},$$

where  $r_{ij} \in \{0, 1\}$ ,  $i, j = 1, 2, 3$ . Let  $\mathcal{T} = G\tilde{\mathcal{T}}$ . We introduce the map  $\varkappa$  of  $\mathcal{T}$  to a set  $\varkappa\mathcal{T}$  as follows:

$$\varkappa: \begin{pmatrix} r_{11} & r_{12} & r_{13} \\ r_{21} & r & r_{23} \\ r_{31} & r_{r32} & r_{33} \end{pmatrix} \rightarrow \begin{pmatrix} r_{11} & r_{12} & r_{13} \\ r_{21} & 1 \oplus r & r_{23} \\ r_{31} & r_{32} & r_{33} \end{pmatrix}, \tag{46}$$

where  $1 \oplus r = 1 + r \pmod{2}$ . For any tile  $\bar{r}$  let  $q(\bar{r})$  be a  $5 \times 5$  matrix such that  $\bar{r}$  is the central tile of  $q(\bar{r})$ . More precisely, let

$$q(\bar{r}) = \begin{pmatrix} q_{11} & \cdots & q_{15} \\ \cdots & & \\ q_{51} & \cdots & q_{55} \end{pmatrix},$$

where  $q_{ij} \in \{0, 1\}$ . Then  $q_{ij} = r_{i-1j-1}$  for  $2 \leq i, j \leq 4$ . The energy of  $q(\bar{r})$  is

$$H(q(\bar{r})) = \sum_{\bar{p} \subseteq q(\bar{r})} \Phi(\bar{p}),$$

where  $\bar{p}$  is a tile and  $\bar{p} \subseteq q(\bar{r})$  means that  $\bar{p}$  is a tile which is included into  $q(\bar{r})$ . Obviously there are 9 tiles included into  $q(\bar{r})$ .

Assume that

**R1.** for any  $\bar{r} \in \mathcal{T}$  and any  $q(\bar{r})$

$$H(q(\bar{r})) \geq H(q(\varkappa\bar{r})). \tag{47}$$

Then

**Theorem 7.** Any model of  $\mathfrak{M}$  satisfying the condition **R1** is regular.

The next theorem must provide another condition ensuring the regularity:

**Theorem 8.** Assume that for a model of  $\mathfrak{M}$  the following inequality holds

$$c_1 = \max_{\bar{u} \in \mathcal{U}} \{\Phi(\bar{u})\} < c_2 = \min_{\bar{r} \notin \mathcal{U}} \{\Phi(\bar{r})\}. \quad (48)$$

If  $c_2 - c_1$  is large enough then the model is regular.

## APPENDIX A: PROOF OF LEMMA 5

We assume that the splitting contour  $\Gamma_x$  of a configuration  $\mathbf{x} \in \mathbf{X}_V(\sigma)$  is an arbitrary regular one. We find a configuration  $\mathbf{x}_0$  such that  $H(\mathbf{x}_0) \leq H(\mathbf{x})$ , the slope of  $\mathbf{x}_0$  is equal to the slope of  $\mathbf{x}$ , that is  $\mathbf{x}_0 \in \mathbf{X}_V(\sigma)$ , and  $\Gamma_{\mathbf{x}_0}$  is canonical.

Finding  $\mathbf{x}_0$  we apply to  $\mathbf{x}$  a number of transformations which do not increase the energy. To describe the transformations we introduce several notions and notations. For integer  $N_1, N_2, M_1, M_2$  let

$$V_{-N_1, N_2}^{-M_1, M_2} = \{(t_1, t_2) \in \mathbb{Z}^2: -N_1 \leq t_1 \leq N_2, -M_1 \leq t_2 \leq M_2\}$$

When  $N = N_1 = N_2 = M_1 = M_2$  we shall use the notation  $V_N = V_{-N, N}^{-N, N}$  as before. We use  $V$  to denote  $V_{-N_1, N_2}^{-M_1, M_2}$  when the values of integers  $N_1, N_2, M_1$  and  $M_2$  are either fixed or not important.

### A.1. Rebuilding 1

First we construct transformations taking  $\mathbf{x}$  to  $\mathbf{x}_1$ . The new configuration  $\mathbf{x}_1$  has a monotone splitting contour  $\Gamma_{\mathbf{x}_1}^*$  and is defined on a volume  $V_{-N, N_2}^{-N_1, N}$  including  $V_N$ . The slope of  $\mathbf{x}_1$  will be greater than the slope  $\sigma$  of  $\mathbf{x}$ , and  $H(\mathbf{x}) = H(\mathbf{x}_1) + O(1)$ .

**Lemma 9.** Let  $\mathbf{x} \in \mathbf{X}_{V_N}(\sigma)$  be a regular configuration. Assume that  $\mathcal{E}_x = \Gamma_x$ . Then there exists a configuration  $\mathbf{x}_2$  on some volume  $V_{-N, N_2}^{-N, N} \supseteq V_N$  such that

1.  $H(\mathbf{x}_2) = H(\mathbf{x})$ ,
2. there is a function  $g$  on  $[-N-1, N_2+1]$  such that  $\Gamma_{\mathbf{x}_2}^*$  is defined by  $g$ .

*Proof.* Using the order in  $\{\Gamma_x^*\}$  we introduce the notion of interval:

$$[(m_1, k_1), (m_2, k_2)] = \{(m, k) \in \{\Gamma_x^*\} : (m_1, k_1) \preceq (m, k) \preceq (m_2, k_2)\}$$

for  $(m_1, k_1) \preceq (m_2, k_2)$ ;  $(m_1, k_1), (m_2, k_2) \in \mathbb{Z}_*^2$ . We also use the notation  $[\cdot, (m, k)]$  ( $[(m, k), \cdot]$ ), where “ $\cdot$ ” means minimal (maximal) site on  $\{\Gamma_x^*\}$ .

For any column  $L_m = \{(m, k) : -N - \frac{1}{2} \leq k \leq N + \frac{1}{2}, k \in \mathbb{Z}_* = \mathbb{Z} + \frac{1}{2}\}$  let  $K_m = L_m \cap \{\Gamma_x^*\}$ . Here  $m \in \mathbb{Z}_*$  and  $-N - \frac{1}{2} \leq m \leq N + \frac{1}{2}$ . A column  $L_m$  is *simple* if  $K_m$  is a one-point set. Let  $L_m$  be not simple. Then the column  $L_m$  contains a *vertical fold*  $F \subseteq K_m$ , if:

1. there exist constants  $k(F)$  and  $\bar{k}(F) \in \mathbb{Z}_*$  such that  $F = [(m, k(F)), (m, \bar{k}(F))]$ ,
2. let  $(\underline{m}, \underline{k}) = \max\{(m', k') \in \{\Gamma_x^*\} : (m', k') \prec (m, k(F))\}$  and  $(\bar{m}, \bar{k}) = \min\{(m', k') \in \{\Gamma_x^*\} : (m', k') \succ (m, \bar{k}(F))\}$  then either

$$\underline{m} = \bar{m} = m - 1 \tag{49}$$

or

$$\underline{m} = \bar{m} = m + 1. \tag{50}$$

It is clear that  $F$  is a maximal connected component in  $K_m$ . (Remark that unlike  $p$ -connection we use here the term connection in the usual geometrical sense).

If all  $L_m, m \in [-N - \frac{1}{2}, N + \frac{1}{2}]$ , are simple then the contour  $\Gamma_x^*$  can be defined by a function  $g$ . Moreover if for any  $m$  such that  $L_m$  is not simple  $L_m$  has no folds then the contour  $\Gamma_x^*$  can be represented by a splitting function  $g$ , as well. In those cases all tiles centered in  $\hat{\Gamma}_x$  belong to  $\mathcal{U}$ .

Let now  $m_0 \in [-N - \frac{1}{2}, N + \frac{1}{2}]$  be the maximal number such that  $L_{m_0+1}$  is simple and  $L_{m_0}$  contains a fold. Since  $m_0$  is maximal then all folds in  $L_{m_0}$  are satisfied (49). Assume that  $F_0$  is the last fold in  $L_{m_0}$ . It means that  $F' \preceq F_0$  for any fold  $F'$  in  $L_{m_0}$ . Let  $m_1 \in \mathbb{Z}$  be minimal such that  $L_{m_1}$  contains a fold  $F_1$  and  $F_1 \succ F_0$ . Let  $F_1$  be maximal satisfied mentioned conditions. The fold  $F_1$  exists since  $F_0$  is the fold having maximal value of abscissa  $m_0$ .

We introduce a transformation  $R$  of  $\Gamma_x^*$  called *double-reflection* as follows: every bond  $b = \langle (m', k')(m'', k'') \rangle$  such that  $(m', k'), (m'', k'') \in [(m_0, k(F_0)), (m_1, \bar{k}(F_1))]$  is taken to  $Rb = \langle (2m_0 - m', k')(2m_0 - m'', k'') \rangle$ . And every bond  $b = \langle (m', k')(m'', k'') \rangle$  such that  $(m', k'), (m'', k'') \in [(m_1, \bar{k}(F_1)), \cdot]$  is taken to  $Rb = \langle (2(m_0 - m_1) + m', k')(2(m_0 - m_1) + m'', k'') \rangle$ . All other bonds of  $\Gamma_x^*$  are not moved. The double-reflection reflects

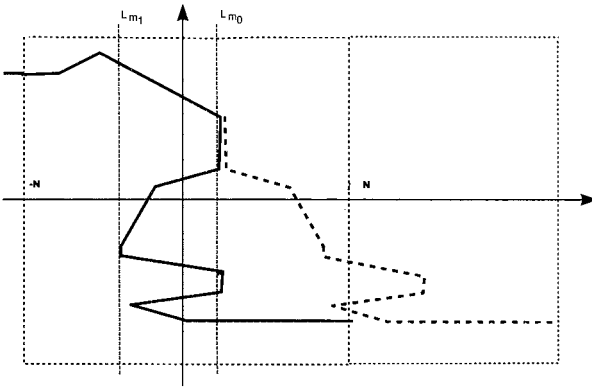


Fig. 3. Double reflection.

$[(m_0, k(F_0)), (m_1, \bar{k}(F_1))]$  with respect to the column  $L_{m_0}$ , and shifts  $[(m_1, \bar{k}(F_1)), \cdot]$  to the right for the distance  $2(m_0 - m_1)$  (see Fig. 3).

It is clear that the set of bonds  $RI_x^*$  is located in the volume  $V_{-N, N}^{-N, N+m_0-m_1} \supseteq V_N$ . Let  $\hat{x}$  be the configuration on  $V_{-N, N}^{-N, N+m_0-m_1}$  such that  $RI_x^*$  is its splitting contour, that is  $\Gamma_{\hat{x}}^* = RI_x^*$ , and  $\Xi_{\hat{x}}^* = \Gamma_{\hat{x}}^*$ .

Further we use the following notations. Let  $B$  be a set of bonds on  $\mathbb{Z}^2$ . Then  $[B] \supseteq \mathbb{R}^2$  is a set of points of  $\mathbb{R}^2$  which either belong to an interval in  $\mathbb{R}^2$  corresponding to a bond  $b \in B$  or are situated in a triangle generated by two bonds  $b_1, b_2 \in B$  having a common site. Let  $V \supseteq \mathbb{Z}^2$  then  $B(V)$  is the set of bonds such that  $b = \langle t_1, t_2 \rangle \in B(V)$  if  $t_1$  and  $t_2 \in V$ .

We now show that the energy of  $\hat{x}$  is equal to the energy of  $x$ . Only tiles  $x_{W_t}$  and  $\hat{x}_{W_s}$  have non-zero energy if  $t \in \hat{\Gamma}_x$  and  $s \in \hat{\Gamma}_{\hat{x}}$ . Therefore our goal is to show that  $H(x_{\hat{f}_x}) = H(\hat{x}_{\hat{f}_x})$ . To this end we part  $\hat{\Gamma}_x$  into several pieces.

Let  $\hat{\Gamma}_x^0 \subseteq \hat{\Gamma}_x$  be such that  $[W_t] \cap [\cdot, (m_0, k(F_0))] \neq \emptyset$  and  $[W_t] \cap [(m_0, k(F_0)), \cdot] = \emptyset$  for any  $t \in \hat{\Gamma}_x^0$ . It means bonds composed by sites of  $\hat{\Gamma}_x^0$  are not moved by the double-reflection. Thus  $x_{W_t} = \hat{x}_{W_t}$  and the energy of those part of the contour is not changed.

Next we consider a set  $\hat{\Gamma}_x^1$  such that  $t \in \hat{\Gamma}_x^1$  if  $(m_0, \bar{k}(F_0)) \in [W_t]$ . Then there are four sites composing  $\hat{\Gamma}_x^1$ :

$$\{(m_0 \pm \frac{1}{2}, \bar{k}(F_0) \pm \frac{1}{2})\}.$$

We use the notation  $t_{\varepsilon_1, \varepsilon_2} = (m_0 \varepsilon_1 \frac{1}{2}, k_0 \varepsilon_2 \frac{1}{2})$ , where  $\varepsilon_1, \varepsilon_2 \in \{+, -\}$ . Let us consider an example to show that the energy before and after the

double-reflection are the same. We consider two sites  $t_{--}$  and  $t_{+-}$  and corresponding tiles

$$W_{t_{--}} = \begin{pmatrix} 0 & 0 & 1 \\ 0 & 1 & 1 \\ r & 1 & 1 \end{pmatrix}, \quad W_{t_{+-}} = \begin{pmatrix} 0 & 1 & 1 \\ 1 & 1 & 1 \\ 1 & 1 & 1 \end{pmatrix}$$

before the double-reflection. Here  $r \in \{0, 1\}$  depends on the contour  $\Gamma_x$ . We have the tiles shown above because of the contour regularity. After the double-reflection we obtain the following tiles

$$RW_{t_{--}} = \begin{pmatrix} 0 & 0 & 1 \\ 0 & 0 & 0 \\ 0 & 0 & 0 \end{pmatrix}, \quad RW_{t_{+-}} = \begin{pmatrix} 0 & 1 & 1 \\ 0 & 0 & 1 \\ 0 & 0 & q \end{pmatrix},$$

where  $q = 1 - r$ . We used the same symbol  $R$  applied to site transformation. It is evident that

$$\Phi(W_{t_{--}}) + \Phi(W_{t_{+-}}) = \Phi(RW_{t_{--}}) + \Phi(RW_{t_{+-}}).$$

We denote the next piece of  $\hat{F}_x$  by  $\hat{F}_x^2$  which is defined such that  $[B(\hat{F}_x^2)] \cap [(m_0, \bar{k}(F_0)), (m_1, \bar{k}(F_1))] \neq \emptyset$ , and  $(m_0, \bar{k}(F_0)) \notin [W_t]$  and  $(m_1, \bar{k}(F_1)) \notin [W_t]$  for any  $t \in \hat{F}_x^2$ . It follows from the regularity that if

$t \in \hat{F}_x^2$  then  $W_{Rt} \cap \hat{F}_x = \emptyset$  and  $W_t \cap \hat{F}_x = \emptyset$ . Moreover if  $\mathbf{x}_{W_t} = \begin{pmatrix} r_{11} & r_{12} & r_{13} \\ r_{21} & r_{22} & r_{23} \\ r_{31} & r_{32} & r_{33} \end{pmatrix}$

for  $\hat{F}_x^2$  then  $\hat{\mathbf{x}}_{W_{Rt}} = \begin{pmatrix} 1-r_{13} & 1-r_{12} & 1-r_{11} \\ 1-r_{23} & 1-r_{22} & 1-r_{21} \\ 1-r_{33} & 1-r_{32} & 1-r_{31} \end{pmatrix}$ . It is clear from the above properties that the energies of  $\mathbf{x}_{\hat{F}_x^2}$  and  $\hat{\mathbf{x}}_{R\hat{F}_x^2}$  are the same.

The next piece  $\hat{F}_x^3$  of  $\hat{F}_x$  is defined by the following relation

$$[W_t] \cap [(m_1, \bar{k}(F_1)), \cdot] \neq \emptyset$$

for  $t \in \hat{F}_x^3$ . The energies of  $\mathbf{x}_{W_t}$  and  $\hat{\mathbf{x}}_{W_{Rt}}$  are the same because  $\hat{\mathbf{x}}_{W_{Rt}}$  is a shift of  $\mathbf{x}_{W_t}$ .

It is clear that the fold  $F_0$  in the column  $L_{m_0}$  is removed by  $R$ . The configuration  $\hat{\mathbf{x}}$  is defined on the volume  $V_{-N, N'}^{-N, N}$ , where  $N' - N$  is a value of the shift of the double-reflection determined above.

After a finite number of double-reflections corresponding to different vertical folds of  $\mathbf{x}$  we obtain a configuration  $\mathbf{x}_2$  without the vertical folds,

and which is defined on a volume  $V_{-N, N_2}^{-N, N}$  where  $N_2 - N$  is the total shift which appears by folds removing. Then there is a function  $g$  defining the splitting contour  $\Gamma_{x_2}^*$ . It is clear that the energy of  $x_2$  is equal to the energy of  $x$ . ■

The configuration  $x_2$  has no vertical folds. Next we construct a configuration  $x_1$  having a monotone splitting contour, that is we eliminate all folds.

**Lemma 10.** There exists a configuration  $x_1$  on a volume  $V_{-N, N_2}^{-N_1, N}$  containing  $V_{-N, N_2}^{-N, N}$  such that

1.  $H(x_2) = H(x_1)$ ,
2. there is a monotone function  $h$  on  $[-N-1, N_2+1]$  such that  $\Gamma_{x_1}$  is defined by  $h$ .

*Proof.* We consider rows  $M_m = \{(k, m) : k \in [-N-1, N_2+1]\} \subset \mathbb{Z}_*$ , for  $m \in \mathbb{Z}_*$ . In the case  $K_m = M_m \cap \{\Gamma_{x_2}^*\} \neq \emptyset$  we call  $m$  simple if  $K_m$  is one-point set. If  $K_m$  is not simple then it is composed of connected components. Let  $F \subseteq K_m$  a connected component having more than one point. Let  $k(F)$  be such that  $(k(F), m) = \min\{(k, m) \in F\}$  and similarly let  $\bar{k}(F)$  be such that  $(\bar{k}(F), m) = \max\{(k, m) \in F\}$ . Let  $(\underline{k}, \underline{m}) = \max\{(k', m') \in \{\Gamma_{x_2}^*\} : (k', m') < (k(F), m)\}$  and  $(\bar{k}, \bar{m}) = \min\{(k', m') \in \{\Gamma_{x_2}^*\} : (k', m') > (\bar{k}(F), m)\}$ .

A connected component  $F \subseteq K_m$  is a *horizontal fold* if  $\underline{m} = \bar{m}$ .

If a contour  $\Gamma_{x_2}^*$  is determined by a function  $g$  and there is no folds then  $g$  is monotone.

Assume next that  $m_0$  is maximal such that  $K_{m_0}$  includes a fold. For any fold in  $K_{m_0}$  we have  $\bar{m}_0 = \underline{m}_0 = m_0 - 1$ . Let  $m_1$  be minimal such that  $K_{m_1}$  includes a fold and  $B(K_{m_1}) \leq B(K_{m_0})$ . The existence of such  $m_1$  is a consequence of the existence of  $m_0$ . It follows from the minimality of  $m_1$  that  $\bar{m}_1 = \underline{m}_1 = m_1 + 1$  for any fold in  $K_{m_1}$ . Let  $F_0$  a minimal fold on  $K_{m_0}$  and  $F_1$  be a maximal fold on  $K_{m_1}$ .

We introduce a transformation  $R$  called *double-reflection*. The usage of the same term that we introduced in Lemma 9 will not lead to a confusion because we use only last notion in this proof. The double reflection reflects the piece  $[(\bar{k}(F_1), m_1), (\bar{k}(F_0), m_0)]$  of  $\{\Gamma_{x_2}^*\}$  with respect to the row  $M_{m_1}$ , and shifts the part  $[(\bar{k}(F_0), m_0), \cdot]$  of the contour down with the distance  $2(m_0 - m_1)$ . The other part of the contour is not moved. The configuration  $\hat{x}$  such that  $\Gamma_{\hat{x}}^* = R\Gamma_{x_2}^*$  is defined on the volume  $V_{-N, N_2}^{-N-2(m_0-m_1), N}$ , where  $N_2$  is defined in Lemma 9 proof.

The double-reflection removes  $F_0$ . Remark that the row  $M_{m_0}$  can include several folds. The equality  $H(x_2) = H(\hat{x})$  can be proved in the same way as it was done in Lemma 9.

Iterating the above construction we obtain a configuration  $x_1$  with a splitting contour defined by a monotone function having its energy equal to  $x_2$ . ■

Remark that  $b^{\text{out}}$  of  $x_1$  is shifted down with the respect to  $b^{\text{out}}$  of  $x_2$  by  $N_1 - N$ . Hence the slope of  $x_1$  is

$$\sigma_1 = \frac{(2\sigma - 1)N + N_1}{N + N_2 + 2}. \quad (51)$$

## 5.2. Rebuilding 2

Next we rebuild the configuration  $x_1$  to the canonical shape.

**Lemma 11.** For any configuration  $y$  having a monotone splitting contour there exists a configuration  $z$  defined in the same volume and with the same slope as  $y$  and such that

1.

$$H(z) \leq H(y) + O(1) \quad (52)$$

when  $N \rightarrow \infty$ .

2. The splitting contour  $\Gamma_z^*$  of  $z$  is canonical.

*Proof.* We represent a monotone decreasing contour  $\Gamma_y^*$  as a sequence of  $+1$ 's and  $-1$ 's. We assign  $+1$  to every horizontal bond  $b^* \in \Gamma_y^*$  and  $-1$  to every vertical bond of  $\Gamma_y^*$ . Because of the regularity of contours only 14 of 16 4-tuples sequences can be met in this representation of the contour. Namely, there are the following 7 4-tuples sequences

$$\begin{aligned} +1+1+1+1, \quad +1+1-1+1, \quad +1+1+1-1, \quad -1+1+1+1, \\ +1-1+1+1, \quad -1+1+1-1, \quad -1+1-1+1, \end{aligned} \quad (53)$$

and sequences obtained from the above by flipping  $+1$  to  $-1$  and vice versa. The energy of every 4-tuple in (53) is a sum of energy of two tiles. It is

$$\begin{aligned}
E(+1+1+1+1) &= \Phi \begin{pmatrix} 1 & 1 & 1 \\ 1 & 1 & 1 \\ 0 & 0 & 0 \end{pmatrix} + \Phi \begin{pmatrix} 1 & 1 & 1 \\ 0 & 0 & 0 \\ 0 & 0 & 0 \end{pmatrix} \\
E(+1+1-1+1) = E(+1-1+1+1) &= \Phi \begin{pmatrix} 1 & 1 & 1 \\ 1 & 1 & 1 \\ 0 & 1 & 1 \end{pmatrix} + \Phi \begin{pmatrix} 1 & 1 & 1 \\ 0 & 0 & 1 \\ 0 & 0 & 0 \end{pmatrix} \\
E(+1+1+1-1) = E(-1+1+1+1) &= \Phi \begin{pmatrix} 1 & 1 & 1 \\ 1 & 1 & 1 \\ 0 & 0 & 1 \end{pmatrix} + \Phi \begin{pmatrix} 1 & 1 & 1 \\ 0 & 0 & 0 \\ 0 & 0 & 0 \end{pmatrix} \quad (54) \\
E(-1+1+1-1) &= 2\Phi \begin{pmatrix} 1 & 1 & 1 \\ 1 & 1 & 1 \\ 0 & 0 & 1 \end{pmatrix} \\
E(-1+1-1+1) &= \Phi \begin{pmatrix} 1 & 1 & 1 \\ 1 & 1 & 1 \\ 0 & 1 & 1 \end{pmatrix} + \Phi \begin{pmatrix} 1 & 1 & 1 \\ 0 & 1 & 1 \\ 0 & 0 & 1 \end{pmatrix}.
\end{aligned}$$

We rebuild  $\Gamma_y^*$  to a canonical form using the new representation.

The monotone canonical contour is divided into 5 pieces. We list below all the pieces from the left side of  $\bar{V}$  to the right one by showing 2-tuples or 3-tuples which compose pieces.

1. Piece 1 is composed by 2-tuples  $+1+1$
2. Piece 2 is composed by 3-tuples  $-1+1+1$
3. Piece 3 is composed by 2-tuples  $-1+1$
4. Piece 4 is composed by 3-tuples  $-1-1+1$
5. Piece 5 is composed by 2-tuples  $-1-1$

We recall that  $+1$  is assigned to the most left bond  $b^{*\text{in}}$  of  $\Gamma_y^*$  (see (25)).

We rebuild  $\Gamma_y^*$  such that a new contour will be canonical, monotone and connect  $b^{*\text{in}}$  and  $b^{*\text{out}}$ . The energy of the new contour differs from the energy of  $\Gamma_y^*$  by a constant for all  $N$ .

We fix a string of  $+1$ 's starting from the left, namely, from  $b^{*\text{in}}$ . It is a part of Piece 1. Then we find every sequence of the kind:

$$\sigma = -1+1+1 \cdots +1-1, \quad (55)$$

where a number  $p$  of  $+1$ 's between two  $-1$ 's is greater than 2. We replace  $p-2$  of  $+1$ 's to Piece 1 such that we obtain the 4-tuple  $-1+1+1-1$



instead of  $\sigma$ . The string of  $+1$ 's having its length  $p-2$  is joined to the left shell of  $+1$ 's. The energy of  $\sigma$ , is

$$E(\sigma) = \Phi \begin{pmatrix} 0 & 1 & 1 \\ 0 & 0 & 0 \\ 0 & 0 & 0 \end{pmatrix} + \Phi \begin{pmatrix} 1 & 1 & 1 \\ 1 & 1 & 1 \\ 0 & 0 & 0 \end{pmatrix} + \Phi \begin{pmatrix} 1 & 1 & 1 \\ 0 & 0 & 0 \\ 0 & 0 & 0 \end{pmatrix} + \dots \\ + \Phi \begin{pmatrix} 1 & 1 & 1 \\ 0 & 0 & 0 \\ 0 & 0 & 0 \end{pmatrix} + \Phi \begin{pmatrix} 1 & 1 & 1 \\ 1 & 1 & 1 \\ 0 & 0 & 1 \end{pmatrix}.$$

By the replacement we obtain the energy of the 4-tuple  $-1+1+1-1$

$$E(-1+1+1-1) = \Phi \begin{pmatrix} 0 & 1 & 1 \\ 0 & 0 & 0 \\ 0 & 0 & 0 \end{pmatrix} + \Phi \begin{pmatrix} 1 & 1 & 1 \\ 1 & 1 & 1 \\ 0 & 0 & 1 \end{pmatrix}.$$

Let  $\Gamma_{y_1}^*$  be a new contour with a corresponding configuration  $y_1$ . If the bond next to the right of  $b^{*in}$  is horizontal (that is it has  $+1$ ) then the energy contours  $\Gamma_y^*$  and  $\Gamma_{y_1}^*$  are the same. Otherwise the energy of  $\Gamma_y^*$  and  $\Gamma_{y_1}^*$  can be different. There are three places in  $y_1$ , where the energy might be changed. Namely, it is the place in  $\Gamma_y^*$ , where  $y$  was cut (to the right of  $b^{*in}$ ) and two places in  $\Gamma_{y_1}^*$ , where a string of  $+1$ 's having its length equal to  $p-2$  was sewed in.

Consequent applications of this rebuilding give a new contour  $\Gamma_{y_k}^*$  with a corresponding configuration  $y_k$  such that Piece 1 composition is completed, that is there are no strings of  $+1$ 's longer than 2 in the last part of  $\Gamma_{y_k}^*$ . The difference of the energy between  $y$  and  $y_k$  is the same as between  $y$  and  $y_1$ .

We obtain piece 5 composed by  $-1$ 's in the similar way by rebuilding strings  $+1-1 \dots -1+1$  to the left of  $b^{*out}$ .

Next we construct Piece 2. The piece must be a periodical sequence

$$+1+1-1+1+1-1+1+1-1\dots,$$

where the first two elements  $+1+1$  belong to the first piece (if it exists). It might not be the first  $+1+1$ . Then we have a contribution to  $O(1)$ . Assume we have a similar sequence attached to the right end of Piece 1. Then we have the following string

$$+1+1-1 \Big| +1-1 \tag{56}$$

on the right end of this sequence. The first three elements belong to Piece 2 we are constructing. The sign  $\mid$  means the end of a part of Piece 2 that exists at the moment. Next we are looking for the first string  $+1+1-1$  to the right of (56). Assume there exists a periodical string of the kind

$$+1+1-1+1+1-1\cdots+1+1-1$$

which is located to the right of (56) on some distant from it. Then we replace this string and attach it to the right end of Piece 2, before the sign  $\mid$  (see (56)). We have to show that the energies of the contours before and after the replacement are the same. To this end we check that changes of the energy do not occur at the points where the contours were cut and sticked.

Let

$$\cdots+1+1-1\alpha_1\alpha_2\alpha_3\cdots\beta_1\beta_2\beta_3+1+1-1\cdots+1+1-1\gamma_1\gamma_2\gamma_3\cdots \quad (57)$$

be the contour before the replacement, and

$$\cdots+1+1-1+1+1-1\cdots+1+1-1\alpha_1\alpha_2\alpha_3\cdots\beta_1\beta_2\beta_3\gamma_1\gamma_2\gamma_3\cdots \quad (58)$$

be the contour that is obtained after the replacement. We have to evaluate the energy of  $\beta_1\beta_2\beta_3\gamma_1\gamma_2\gamma_3$  and  $+1+1-1+1+1-1$  and compare it with the energy of  $\beta_1\beta_2\beta_3+1+1-1$  and  $+1+1-1\gamma_1\gamma_2\gamma_3$ . Remark that  $\alpha_1 = +1$  and  $\alpha_2 = -1$ . Because of the contour regularity, it is impossible that  $\alpha_1 = -1$ . The value of  $\alpha_3$  can be arbitrary. By the same reasons and because we have no sequences  $+1+1+1\cdots$  in the studied piece of the contour we obtain that  $\beta_2 = +1$ ,  $\beta_3 = -1$ . Recall that  $+1$  or  $-1$  are assigned to bonds. Let  $b(\delta)$ , where  $\delta \in \{+1, -1\}$ , be a bond having  $\delta$  assigned to it. Because  $b(\beta_1) < b(\beta_3)$  we have  $\beta_1 = -1$ , otherwise the sequence  $+1+1-1$  occurs earlier than we assumed. Also  $\gamma_1 = +1$ ,  $\gamma_2 = -1$  and  $\gamma_3$  is arbitrary. Hence (57) and (58) are

$$\cdots+1+1-1\mid+1-1\alpha_3\cdots-1+1-1\mid+1+1-1\cdots+1+1-1\mid+1-1\gamma_3\cdots \quad (59)$$

$$\cdots+1+1-1\mid+1+1-1\cdots+1+1-1\mid1-1\alpha_3\cdots-1+1-1\mid+1-1\gamma_3\cdots \quad (60)$$

We show now that the energy of (59) and (60) are equal. To this end we have to compare the energies of strings around vertical delimiters in (59) and (60). We consider three strings

$$+1+1-1+1-1\alpha_3, \quad -1+1-1+1+1-1, \quad \text{and} \quad +1+1-1+1-1\gamma_3 \tag{61}$$

in (59) and three strings

$$+1+1-1+1+1-1, \quad -1+1-1+1-1\alpha_3, \quad \text{and} \quad -1+1-1+1-1\gamma_3 \tag{62}$$

in (60). Using (54), by direct calculations we obtain that the energy of three strings in (61) is equal to the energy of the three strings in (62).

The similar procedure gives Piece 4 of the canonical contour composed by strings  $-1-1+1$ . We obtain Piece 3 composed by string  $+1-1$  automatically. ■

Applying the Lemma 11 to the configuration  $\mathbf{x}_1$  we obtain a configuration  $\tilde{\mathbf{x}}_1$ , having a monotone canonical contour and such that the energy of the original configuration  $\mathbf{x}$  and of  $\tilde{\mathbf{x}}_1$  differ by a fixed constant for all  $N$ . The volume where  $\tilde{\mathbf{x}}_1$  is defined is  $V_{-N, N_1}^{-N, N_2}$  with  $N_1, N_2 \geq N$ . The slope of  $\Gamma_{\tilde{\mathbf{x}}_1}^*$  is  $\tilde{\sigma}_1 = \sigma_1$  (see (51)).

We introduce notations used in the next section. Let  $t_I = -N - \frac{3}{2}$  and let  $t_{II} \in \mathbb{Z}_*$  be the point where Piece 1 and Piece 2 of  $\Gamma_{\tilde{\mathbf{x}}_1}^*$  join. If Piece 1 is empty then  $t_{II} = -N - \frac{1}{2}$ . The point  $t_{III}$  is the join point of Piece 2 and Piece 3. If Piece 2 is empty then  $t_{II} = t_{III}$ . The point  $t_{IV}$  is the join point of Piece 3 and Piece 4. If Piece 3 is empty then  $t_{III} = t_{IV}$ . Let  $t_V = N_1 + \frac{1}{2}$ .

### 5.3. Rebuilding 3

In the previous steps we changed the contour  $\Gamma_{\mathbf{x}}^*$  such that in the new now canonical contour  $\Gamma_{\tilde{\mathbf{x}}_1}^*$  output bond is on a level which is less than  $-\sigma N$ .

**Lemma 12.** Let  $\Gamma^*(1)$  be a canonical contour in a volume  $V = V_{-K_1, K_2}^{-M_1, M_2}$   $M_1, M_2, K_1, K_2 \in \mathbb{Z}$  defined by a monotone decreasing splitting function  $g_1$ . Let  $b^{\text{in}}(1) = \langle t_1^{\text{in}}(1), t_2^{\text{in}}(1) \rangle$  and  $b^{\text{out}}(1) = \langle t_1^{\text{out}}(1), t_2^{\text{out}}(1) \rangle$  be input and output bonds of  $\Gamma^*(1)$ , and  $\sigma(1) = \frac{t_2^{\text{out}}(1) - t_2^{\text{in}}(1)}{t_1^{\text{in}}(1) - t_1^{\text{out}}(1)}$ .

Then for any  $\sigma : 0 < \sigma \leq \sigma(1)$  there exists a canonical contour  $\Gamma^*(2)$  (may be not monotone) such that

1.  $b^{\text{in}}(1) = b^{\text{in}}(2)$ ,  $t_1^{\text{out}}(1) = t_1^{\text{out}}(2)$ ,  $t_2^{\text{out}}(1) \geq t_2^{\text{out}}(2)$  and  $\sigma(2) = \frac{t_2^{\text{out}}(2) - t_2^{\text{in}}(2)}{t_1^{\text{in}}(2) - t_1^{\text{out}}(2)}$ , where  $b^{\text{in}}(2) = \langle t_1^{\text{in}}(2), t_2^{\text{in}}(2) \rangle$  and  $b^{\text{out}}(2) = \langle t_1^{\text{out}}(2), t_2^{\text{out}}(2) \rangle$  are input and output bonds of  $\Gamma^*(2)$ .

2. If  $y_1$  and  $y_2$  are configurations on  $V$  having  $\Gamma^*(1)$  and  $\Gamma^*(2)$  as contours then

$$H(y_1) \leq H(y_2) + O(1) \quad (63)$$

*Proof.* We use the notion of pieces of  $\Gamma^*(1)$  as it was considered in Lemma 11 and in its proof (see also the end of Section 6.2).

The lemma conditions give  $t_1^{\text{out}}(1) = t_2^{\text{out}}(2) = K_2 + \frac{1}{2}$  and  $t_2^{\text{out}}(1) = K_2 + \frac{3}{2}$ . Let  $b_0 = \langle (K_2 - \frac{1}{2}, t_0), (K_2 + \frac{1}{2}, t_0) \rangle \in \Gamma^*(1)$  be a bond intersecting the column  $L_{K_2} = \{(K_2, k) : k \in [-K_1, K_2] \in \mathbb{Z}\}$ . If Piece 5 of  $\Gamma^*(1)$  is not empty then  $b_0$  is the last bond of Piece  $l$ , where  $l$  is the maximal number of existing Pieces not greater than 4 (see the proof of Lemma 11). In this case  $t_0 > t_2^{\text{out}} + 2$ . We assume that the splitting function  $g_1$  on  $[K_2, K_2 + 1]$  in the considered case is:

$$g_1(t) = -(t_0 - t_2^{\text{out}})(t - K_2) + t_0. \quad (64)$$

We apply an algorithm to modify  $\Gamma^*(1)$  such that the resulting contour  $\Gamma^*(2)$  has the same or less energy and  $\sigma(2) = \sigma$ . The algorithm is such that we change slopes of some parts of  $\Gamma^*(1)$ . First we change the direction of angle of a part of Piece 2. Namely, we take the slope of this changed part equal to  $+\frac{1}{2}$  instead of  $-\frac{1}{2}$  that it had. Doing so we take  $s \in [t_{II}, t_{III}] \subset \mathbb{Z}_*$ , and a new contour  $\Gamma_s^*$  is defined by the following function  $g_s$

$$g_s(t) = g(t) \quad \text{for all } t \leq t_{II},$$

$$\frac{dg_s}{dt}(u) = \begin{cases} \frac{1}{2} & \text{if } u \in [t_{II}, s], \\ \frac{dg}{dt}(u), & \text{if } u > s. \end{cases}$$

A new slope  $\sigma_{\Gamma_s^*}$  is less than  $\sigma_{\Gamma^*(1)}$ .

Remark that the energy of the configurations  $y_1$  and a new configuration  $y_s$  having  $\Gamma_s^*$  as splitting contour differed by a constant independent on  $\sqrt{V}$ . The difference arises because of perturbations on the ends of  $[t_2^{\text{out}}, t_2^{\text{in}}] = [t_{II}, s]$ .

If  $\sigma_{\Gamma_s^*} = \sigma$  for some  $s \in [t_{II}, t_{III}]$  then we obtain the canonical contour  $\Gamma_s^*$  which we looked for. Assume next that for  $s = t_{III}$  we have  $\sigma_{\Gamma_s^*} > \sigma$ .

Then we reconstruct Piece 3 having slope  $-1$ . Let  $s \in [t_{III}, t_{IV}]$ . Now a new contour  $\Gamma_s^*$  is defined by a splitting function  $g_s$  such that

$$g_s(t) = g(t) \quad \text{for all } t \leq t_{II},$$

$$\frac{dg_s}{dt}(u) = \begin{cases} \frac{1}{2}, & \text{if } u \in [t_{II}, t_{III}], \\ 1, & \text{if } u \in [t_{III}, s], \\ \frac{dg}{dt}(u), & \text{if } u > s. \end{cases}$$

If for some  $s$  we obtain  $\sigma_{\Gamma_s^*} = \sigma$  then  $\Gamma_s^*$  is the canonical contour we look for. If for  $s = t_{IV}$  we have  $\sigma_{\Gamma_s^*} > \sigma$  then we have to continue similar reconstruction by applying it to Piece 4. Now, however, obtained contours are not canonical. Let  $s \in [t_{IV}, t_V]$  then  $\sigma_{\Gamma_s^*}$  is corresponding to the splitting function

$$g_s(t) = g(t) \quad \text{for all } t \leq t_{II}, \quad (65)$$

$$\frac{d}{dt}g_s(u) = \begin{cases} +\frac{1}{2}, & \text{if } u \in [t_{II}, t_{III}], \\ +1, & \text{if } u \in [t_{III}, t_{IV}], \\ +2, & \text{if } u \in [t_{IV}, s] \\ \frac{d}{dt}g(u), & \text{otherwise} \end{cases} \quad (66)$$

The reconstruction changes the energy for a constant independent on  $\sqrt{V}$ . Let  $\sigma_{\Gamma_s^*} = \sigma$  for some  $s \in [t_{IV}, t_V]$ . The contour  $\Gamma_s^*$  is not canonical since there is a piece of the contour on the interval  $[t_{IV}, s]$  having its slope equal to  $+2$ . To obtain a canonical contour we change  $g_s$ . Let  $h(u) = \frac{1}{2}(u - t_{IV}) + g_s(t_{IV})$  for  $u \geq t_{IV}$ , then a new splitting function  $\tilde{g}_s$  is

$$\tilde{g}_s(u) = \begin{cases} g_s(u), & \text{if } u \leq t_{IV}, \\ \min\{h(u), g_s(u)\}, & \text{if } u > t_{IV}. \end{cases}$$

Let  $\tilde{\mathbf{y}}$  be the configuration on  $V$  defined by  $\tilde{g}_s$  and  $\tilde{\Gamma}^*$  be the corresponding dual splitting contour. We show that  $H(\tilde{\mathbf{y}}) \leq H(\mathbf{y}_{g_s}) + O(1)$ , where  $\mathbf{y}_{g_s}$  is the configuration defined by  $g_s$ . Recall that the order of values of  $H(\tilde{\mathbf{y}})$  and  $H(\mathbf{y}_{g_s})$  is  $N$ . We have to consider two cases. It is clear that there is a solution  $u_0$  of the equation  $h(u) = g_s(u)$  on the interval  $(t_{IV}, t_V + \frac{1}{2}]$ , recall that  $t_V = K_2 + \frac{1}{2}$ .

The first case is  $\frac{d}{dt}g_s(u_0) = -2$ . It means that the line  $h(u)$  intersects Piece 4. Then  $u_0 = \frac{8}{5}s - \frac{3}{5}t_{IV}$ , and the main term of  $H(y_{g_s}) - H(\tilde{y})$  is

$$\frac{16}{5}(s - t_{IV})E_{1/2} > 0.$$

The new contour  $\tilde{\Gamma}^*$  can be reconstructed to a canonical one.

The second case is  $\frac{d}{dt}g(u_0) < -2$ . It means that the line  $h(u)$  intersects Piece 5. Then the main term of  $H(y_{g_s}) - H(\tilde{y})$  is greater than or equal to

$$(t_V - t_{IV})E_{1/2} > 0.$$

Next assume that  $\sigma_{\Gamma_s^*} > \sigma$  for any  $s > t_{IV}$ . Then we use Piece 5 to obtain the needed angle of the slope. We can use the previous considerations to obtain the function  $g_s$  with  $s = t_V$  (see (65)). After we can obtain the function  $\tilde{g}_s$  as in the previous considerations which give the configuration  $\tilde{y}$  with a contour  $\tilde{\Gamma}^*$ . This contour can be altered to a canonical one. To obtain the needed slope  $\sigma$  we change the output bond. Namely, we take  $\tilde{b}^{\text{out}} = (\tilde{t}_1^{\text{out}}, \tilde{t}_2^{\text{out}})$  such that  $\tilde{\sigma}t_2 - t_2^{\text{in}} = \sigma(t_1^{\text{in}} - \tilde{t}_1^{\text{out}})$ . We obtain a new contour  $\Gamma^*(2)$  which is canonical and  $\sigma_{\Gamma^*(2)} = \sigma$ . Let  $y_2$  be the configuration corresponding to  $\Gamma^*(2)$ . ■

Taking  $y_1 = \tilde{x}_1$  in  $V = V_{-N, N_2}^{-N_1, N}$  (see the end of Section 6.2) we obtain as  $y_2$  a configuration  $\hat{x}$  in the same volume with a slope  $\hat{\sigma} \leq \sigma_1$  and such that  $H(\hat{x}_1) \leq H(\tilde{x}) + O(1)$ . We choose  $\hat{\sigma} = \frac{2\sigma N}{N + N_2 + 2}$ . Obviously, the configuration  $\hat{x}$  can be considered in the volume  $V_{-N, N_2}^{-N, N}$ .

Next we show that there exists a configuration  $x_0$  on  $V = V_{-N, N}^{-N, N}$  having a canonical splitting contour such that its energy is less than the energy of  $\hat{x}$  and hence of  $x$ .

The contour of  $x$  is in the volume  $V_{-N, N_2}^{-N_1, N}$  then the tilted boundary conditions around  $V_{-N, N_2}^{-N_1, N}$  is defined by the function

$$x^{\tilde{\sigma}}(t) = \begin{cases} 1, & \text{if } \tilde{\sigma}t_1 + t_2 \geq 0, \\ 0, & \text{otherwise,} \end{cases}$$

where  $\tilde{\sigma} = \frac{\sigma N + N_1}{N + N_2}$ .

First we find a configuration  $\tilde{x}_0$  having the minimal energy in  $Z_{V_{-N, N_2}^{-N, N}}(\tilde{\sigma})$ . The splitting contour of  $\tilde{x}_0$  has a shape which is found by Lemma 4. Now let  $x_0$  be the configuration in  $V = V_{-N, N}^{-N, N}$  having minimal energy in  $Z_V(\sigma)$ . We shall show that

$$H(x_0) \leq H(\tilde{x}_0) \tag{67}$$

Remark that  $\hat{\sigma} \leq \sigma$  therefore (67) is obvious for the case  $\sigma \leq \frac{1}{2}$ . It is also not difficult to understand this fact for the case  $\frac{1}{2} \leq \hat{\sigma}$ . Assume next that  $\hat{\sigma} \leq \frac{1}{2} \leq \sigma$ . Then the inequality (67) is easy to obtain in the regions  $A_{15}$ ,  $A_{17}$ ,  $A_{45}$  because the shape type of the splitting functions for  $\mathbf{x}_0$  and  $\tilde{\mathbf{x}}_0$  are the same. In the region  $[A_{23} \cap A_{36}] \cup [A_{13} \cap A_{36}] \cup [A_{23} \cap A_{35}] \cup [A_{13} \cap A_{35}]$  the shapes of the splitting contours have different types for  $\mathbf{x}_0$  and  $\tilde{\mathbf{x}}_0$ .

In the region  $A_{23} \cap A_{36}$  the splitting function  $\tilde{g}$  of  $\tilde{\mathbf{x}}_0$  is

$$\tilde{g}(-N) = \sigma N, \quad \frac{d}{dt} \tilde{g}(s) = \begin{cases} \frac{1}{2} & \text{if } s \in (-N, \frac{1}{2}(N_2 - N) - 2\sigma N), \\ -\frac{1}{2} & \text{if } s \in (\frac{1}{2}(N_2 - N) - 2\sigma N, N_2), \end{cases} \quad (68)$$

and the splitting function  $g$  of  $\mathbf{x}_0$  is like it is given by (35). Therefore

$$H(\tilde{\mathbf{x}}_0) = (N + N_2) E_{1/2} + O(1), \quad (69)$$

and

$$H(\mathbf{x}_0) = \frac{4}{3} N(1 + \sigma) E_{1/2} + O(1). \quad (70)$$

Since  $\sigma \geq \frac{1}{2}$  we obtain  $4\sigma \geq \frac{4}{3}(1 + \sigma)$ . Besides,  $\hat{\sigma} \leq \frac{1}{2}$  implies that  $\frac{2\sigma N}{N_2 + N} = \frac{2\sigma}{1 + \frac{N_2}{N}} \leq \frac{1}{2}$  or equivalently

$$4\sigma \leq 1 + \frac{N_2}{N}. \quad (71)$$

The last inequality gives (67) for large enough  $N$ .

In the region  $A_{13} \cap A_{36}$

$$\tilde{g}(-N) = \sigma N, \quad \frac{d}{dt} \tilde{g}(s) = \begin{cases} 0 & \text{if } s \in (-N, N_2 - 4\sigma N), \\ -\frac{1}{2} & \text{if } s \in (N_2 - 4\sigma N, N_2). \end{cases} \quad (72)$$

The configuration  $\mathbf{x}_0$  in the considered region is the same as in  $A_{23} \cap A_{36}$  (see (35)). The energy of  $\tilde{\mathbf{x}}_0$  is

$$H(\tilde{\mathbf{x}}_0) = (N_2 + N - 4\sigma N) E_0 + 4\sigma E_{1/2} + O(1). \quad (73)$$

Using (71) we obtain  $N_2 + N - 4\sigma N \geq 0$  hence

$$H(\tilde{\mathbf{x}}_0) \geq 4\sigma N E_{1/2} + O(1). \quad (74)$$

Then (67) holds in  $A_{13} \cap A_{36}$ .

In the region  $A_{23} \cap A_{35}$  the configuration  $\tilde{\mathbf{x}}_0$  is defined by (68) and  $\mathbf{x}_0$  is defined by the splitting function  $g$

$$g(-N) = \sigma N, \quad \frac{d}{dt} g(s) = \begin{cases} -\frac{1}{2} & \text{if } s \in (-N, 3N - 4\sigma N), \\ -1 & \text{if } s \in (3N - 4\sigma N, N). \end{cases} \quad (75)$$

The energy  $H(\tilde{\mathbf{x}}_0)$  is given in (69) and

$$H(\mathbf{x}_0) = 4(1 - \sigma) N E_{1/2} + 2(2\sigma - 1) N E_1 + O(1), \quad (76)$$

(see (36)). We use the inequality  $E_1 \leq \frac{4}{3} E_{1/2}$  which holds in  $A_{35}$ . Then

$$4(1 - \sigma) E_{1/2} + 2(2\sigma - 1) E_1 \leq \frac{4}{3} (1 + \sigma) E_{1/2} \leq 4\sigma E_{1/2} \leq \left(1 + \frac{N_2}{N}\right) E_{1/2}. \quad (77)$$

It gives (67) for large  $N$ .

In the region  $A_{12} \cap A_{35}$  the configurations  $\tilde{\mathbf{x}}_0$  and  $\mathbf{x}_0$  are defined by (72) and (75) accordingly, and the energies of  $\tilde{\mathbf{x}}_0$  and  $\mathbf{x}_0$  are as in (73) and (76). We use (74) and the left inequality in (77) obtaining (67) in this region. ■

## ACKNOWLEDGMENTS

This work was partly supported by the Russian Foundation for Basic Research (Grants 99-01-00003 and 02-01-00068); French-Russian Institute A. M. Liapunov (Grant 98-02); CRDF (Grant RM1-2085)

## REFERENCES

1. X. Descombes and E. Pechersky, *Isotropic Properties of Some Multi-Body Interaction Models: Two Quality Criteria for Markov Priors in Image Processing*, Technical report INRIA, RR-3752, 1999.
2. R. A. Minlos and Ya. G. Sinai, The phenomenon of "phase separation" at low temperatures in some lattice models of a gas I, *Math. USSR-Sb.* 2:337–395 (1967).
3. R. A. Minlos and Ya. G. Sinai, The phenomenon of "phase separation" at low temperatures in some lattice models of a gas II, *Trans. Moscow Math. Soc.* 19:121–196 (1968).
4. R. L. Dobrushin, R. Kotecký, and S. Shlosman, *Wulff Construction: A Global Shape from Local Interaction*, AMS Translations Series, Vol. 104 (Providence, R.I., 1992).
5. T. Bodineau, D. Ioffe, and Y. Velenik, *Rigorous Probabilistic Analysis of Equibrial Crystal Shapes*, Preprint, 2000.
6. J. Besag, Spatial interaction and statistical analysis of lattice systems, *J. Roy. Soc. Ser. B* 48:192–236, 1974.
7. S. Geman and D. Geman, Stochastic relaxation, Gibbs distribution, and the Bayesian restoration of images, *IEEE Trans. on PAMI* 6:721–741, 1984.
8. Ya. G. Sinai, *Theory of Phase Transitions: Rigorous Results* (Pergamon Press, 1982).



9. H-O. Georgii, *Gibbs Measures and Phase Transitions* (Walter de Gruyter, 1988).
10. X. Descombes, J. F. Mangin, E. Pechevsky, and M. Sigelle, Fine structure preserving Markov model for image processing, in *Proc. SCIA* (Uppsala, Sweden, 1995), pp. 349–056.
11. X. Descombes, R. Morris, J. Zerubia, and M. Berthod, Estimation of markov random field prior parameters using Markov Chain Monte Carlo Maximum Likelihood, *IEEE Trans. on Image Processing* **8**:954–963 (1999).
12. X. Descombes and F. Kruggel, A Markov Pixon information approach for low level image description, *IEEE Trans. on Pattern Anaylsis and Machine Intelligence* **21**:482–494 (1999).